A study of diffusion and chemical reactions of ions in pore solution in concrete exposed to chlorides

Johannesson, Björn

2000

LUND INSTITUTE OF TECHNOLOGY
LUND UNIVERSITY

Division of Building Materials

A Study of Diffusion and Chemical Reactions of Ions in Pore Solution in Concrete Exposed to Chlorides

Björn Johannesson

TVBM-3092 Lund 2000

LUND INSTITUTE OF TECHNOLOGY
LUND UNIVERSITY

Division of Building Materials

A Study of Diffusion and Chemical Reactions of Ions in Pore Solution in Concrete Exposed to Chlorides

Björn Johannesson

TVBM-3092 Lund 2000

ISRN LUTVDG/TVBM--00/3092--SE(1-45)
ISSN 0348-7911 TVBM

Lund Institute of Technology
Division of Building Materials
Box 118
SE-221 00 Lund, Sweden

Telephone: 46-46-2227415
Telefax: 46-46-2224427
www.byggnadsmaterial.lth.se

A Study of Diffusion and Chemical Reactions of Ions in Pore Solution in Concrete Exposed to Chlorides

Björn F. Johannesson
Lund Institute of Technology, Division of Building Materials
Box 118, SE-221 00 Lund, Sweden

Abstract

Nearly all deterioration processes in cement-based materials are governed by the conditions in terms of the concentration of different kinds of ions present in the pore solution. Such processes are, for example, chloride-induced reinforcement corrosion, hydroxide ion leaching, carbonation, deicing salt scaling. Here a model will be established accounting for *(i)* diffusion of several common dissolved ions in pore solution, *(ii)* dielectric effects, *(iii)* binding of chlorides and *(iv)* leaching of hydroxide. Experiments are performed on chloride penetration into concretes with three different water to binder ratios. The cement used is a Swedish sulfate-resistant Portland cement, SRPC, trademarked 'anläggningscement'. Silica fume replacing cement by 5 weight percent was used for all three tested concrete qualities.

It is concluded theoretically that the dielectric effect between the diffusing positive and negative ions has considerable effects on the chloride penetration into concrete. Furthermore, by comparing the experimental response with simulations, using the finite element method, it is concluded that the dielectric effect may be one possible explanation for obtaining an *increase* of *total* chloride as a function of the depth from the exposed surface. The maximum total chloride content is often observed a few millimeters from the exposed surface; at greater depths the chloride content gradually decreases as espected. This phenomenon can hardly be explained by simple concentration gradient driven diffusion.

In order to verify the model not only the measured chloride profiles are needed, but also the concentration profiles of all other ions present in pore solution must be evaluated experimentally. This is due to the dielectric diffusion behavior of different types of ions assumed in the model. Here only measurements on chloride profiles are presented. Therefore, this study must be complemented with additional information from measurements in order to confirm the constitutive assumptions in use. Therefore, an extension of this work should be of experimental nature.

A detailed explanation is given for the assumptions leading to the governed equations for the seven constituents considered in the model. Moreover, the structure of the needed numerical treatment of the problem is discussed. The finite element method is used to solve the transient coupled equations. The material constants included in the model are chosen in such a way as to give the best match with the measured chloride profiles.

1 Introduction

A simulation of diffusion and chemical reaction of a system containing 7 different constituents appearing either as dissolved in the pore solution or as being a part of the solid cement hydration products will be performed. The considered constituents being dissolved in the pore solution are: Cl^-, Na^+, OH^-, Ca^{2+} and K^+. The considered solid constituents are $CaCl_2$, and $Ca(OH)_2$ which are assumed to be intergrown with the hydration products of the cement.

The key issue is to establish a model satisfying the physical mass balance laws for the individual constituents, and for the whole mixture. Furthermore, a physical charge balance law will be invoked. This law will serve as an instrument controlling the diffusion of dissolved ions in pore solution in a way that the net charge of ions in every material point is zero or at least very close to zero. The kinetics and equilibrium conditions for the chemical reactions, e.g. binding of chloride ions onto the pore walls and leaching of hydroxide ions from solid to pore solution, will be constituted in a way that the mass balance principals and the charge balance principal are satisfied. The binding of chloride ions will be assumed to be caused by ion exchange with $Ca(OH)_2$ forming $CaCl_2$, with the result that one hydroxide ion is released from solid to the pore solution for every chloride ion that is bound. Moreover, the

dissolution of solid $CaCl_2$ is included in the model. This behavior represents the release of already bound chlorides. The leaching of solid $Ca(OH)_2$ is, simply, assumed as a dissolution in which Ca^{2+} and OH^- are supplied to the pore solution.

The experimental procedure consisted of measuring the chloride ingress for three different types of concretes after 119 days of exposure to a 3 wt.% sodium chloride solution. The cement used was a Swedish sulfate-resistant Portland cement, SRPC (trademarked 'anläggningcement') combined with 5 wt.% silica fume, see table 5. The preparation of samples before exposure to a 3 wt.% sodium chloride solution cosisted of two weeks of storage in air, at room temperature, after casting, followed by one week of submersion in tap water. The water curing before exposure to chloride solution was performed to avoid capillary suction of water containing chlorides. The compressive strength, degree of hydration and active porosity were also measured for the three mixes used.

The total chloride ion content was measured using the Rapid Chloride Test method, RCT. The measured chloride profiles obtained were used together with the established model in order to quantify the introduced material coefficients. The approach was simply to adjust the material parameters to give the best fit with the experimental data.

A finite element scheme has been developed capable of solving the coupled equations describing the diffusion, dielectrics and chemical reactions of the constituents considered. Simple one-dimensional linear spatial elements are used. The time integration scheme used is implicit and unconditionally stable. This becomes necessary since time integration methods, being only conditionally stable, fail due to the time scale and the non-symmetric character of the global 'stiffness' matrix of the problem. The coupling due to dielectric effects and chemical reactions is taken into account by introducing them in the 'stiffness' matrix as off-diagonal block matrixes. By doing this the staggered calculation approach is avoided. Hence all nodal parameters can be evaluated explicitly in one step only, at each time level. This makes the method more robust and reliable compared to a method where each equation is solved one by one together with adjustments of parameters before proceeding to next time level. Non-linearities are present in the problem. These non-linearities are due to the inclusion of dielectric effects among the positive and negative ions in the pore solution. No special numerical treatment is used to minimize errors due to non-linearities, within time steps. The reliability of the solution has, however, been checked by gradually

decreasing the time step length until the solution converges.

By comparing results from experiments and simulation it is concluded that the well-documented experimentally obtained fact that the maximum total chloride concentration in concrete occurs a few millimeters from the exposed surface (still using a constant outer storage concentration of chlorides), can also be obtained theoretically, by analysing the response to simulating the process with the proposed set of governing equations. This is due to the fact that the dielectric effect caused by the mixture of positive and negatively charged ions in the pore solution and chemical reactions between solid hydration products in concrete and the ions in pore solution is considered.

2 Mass balance and the static continuity equation for the ionic charge

In this section the basic physical equations describing balance properties will be introduced. The only balance principles to be used are balance of mass and the continuity equation for the ionic charge. These equations must be supplemented by so-called constitutive relations, or equally material functions, in order to make the number of unknown properties and equations equal. A more simple approach whereby 'convective' velocities are ignored will be used. This means that the velocities of the constituents are assumed to be approximately equal to their corresponding so-called diffusion velocities.

In the so-called mixture theory, e.g. see [1], the mass balance for an individual constituent in a mixture, is the postulate

$$\frac{\partial \rho_a}{\partial t} = -\mathrm{div}\,(\rho_a \dot{\mathbf{x}}_a) + \hat{c}_a; \qquad a = 1, ..., \Re, \tag{1}$$

where ρ_a (kg/m^3) is the mass density of the a:th constituent. The velocity is denoted $\dot{\mathbf{x}}_a$ (m/s), and $\hat{c}_a$ (kg/m^{3}s) the mass gain density to the a:th constituent from all other $\Re - 1$ constituents present in the mixture, where $\Re$ is the number of constituents.

The total mass density of the mixture ρ is by definition

$$\rho = \sum_{a=1}^{\Re} \rho_a \tag{2}$$

One of the cornerstones in the theory of mixtures is that the postulated balance principals for the individual constituents should result in the classical

principals used for single (constituent) materials when summing over all $\Re$ constituents. The postulate for mass balance for a single material is

$$\frac{\partial \rho}{\partial t} = -\text{div}\,(\rho \dot{\mathbf{x}}) \tag{3}$$

where ρ is the mass density of the mixture and $\dot{\mathbf{x}}$ is the mean velocity or simply the velocity of the mixture. By making a summation of all $\Re$ constituent equations in (1) the equation (3) should be the result. This will be the case when defining the mean velocity $\dot{\mathbf{x}}$ as

$$\dot{\mathbf{x}} = \frac{1}{\rho} \sum_{a=1}^{\Re} \rho_a \dot{\mathbf{x}}_a \tag{4}$$

and also by applying the condition

$$\sum_{a=1}^{\Re} \hat{c}_a = 0 \tag{5}$$

This equation states that no net production of mass takes place due to exchange of mass among the constituents in the mixture.

In the application to be presented it will be of interest to use a mol density concentration definition of the constituents, instead of the mass density concentration definition. The relation between the mass density concentration ρ_a and the mol density concentration n_a (mol/m^3) is

$$\rho_a = n_a m_a^c \tag{6}$$

where m_a^c (kg/mol) is the mass of one mol of the a:th constituent. The superscript c is included to stress that this property is constant. During mass exchange among constituents due to, for example, chemical reactions, the total mass is always conserved, i.e. see equation (5), but not necessarily the mol density concentrations. This will in turn mean that a different condition for conservation of mass must be used when using the mol density concentrations as state variables. This condition can easily be derived by considering equation (1) together with the definition (6), as

$$m_a^c \frac{\partial n_a}{\partial t} = -m_a^c \text{div}\,(n_a \dot{\mathbf{x}}_a) + m_a^c \hat{n}_a; \qquad a = 1, ..., \Re, \tag{7}$$

where the mass gain density to the a:th constituent $\hat{c}_a$ is related to the mol gain density $\hat{n}_a$ as: $\hat{c}_a = m_a^c \hat{n}_a$. Summing all $\Re$ constituent equations in (7) should result in equation (3). This implies that the condition

$$\sum_{a=1}^{\Re} m_a^c \hat{n}_a = 0 \tag{8}$$

must hold. The mass balance principals for the constituents to be used is equation (7) rewritten as

$$\frac{\partial n_a}{\partial t} = -\text{div}\,(n_a \dot{\mathbf{x}}_a) + \hat{n}_a; \qquad a = 1, ..., \Re, \tag{9}$$

Equations (8) and (9) will be used together with constitutive equations for the mol density flows and mol density exchange rates for the constituents. The application of diffusion and chemical reactions of ions in pore solution of concrete using constituent equations as described in (9) has been studied in [2].

Mass balance principals can also be expressed in terms of the diffusion velocity $\mathbf{u}_a$, which is defined as the difference between the velocity $\dot{\mathbf{x}}_a$ and the mean velocity $\dot{\mathbf{x}}$, i.e. $\mathbf{u}_a = \dot{\mathbf{x}}_a - \dot{\mathbf{x}}$. This kind of description is often used, for example, when having low mass concentration of dissolved diffusing ions in flowing water. Essentially the water velocity represents the mean velocity $\dot{\mathbf{x}}$; in this case contributing to convection of the dissolved ions.

Yet another balance principle will be invoked since positively and negatively charged ions dissolved in water will be studied. The principal to be used expresses the balance between the space charge density; in this case caused by not having positive and negative ions in solution balancing each other, and the electric displacement field vector. The local statement of the static continuity equation for the charge is one of Maxwell's equations, namely

$$\text{div}\,(\mathbf{d}) = q, \tag{10}$$

where $\mathbf{d}$ is the electric displacement field vector $\mathbf{d}$ (C/m^2) and q (C/m^3) is the space charge density scalar.

3 Constitutive relations

In this section a tentative set of material assumptions will be described. The aim is to specify assumptions which are in accordance with general

experimental observations concerning ion diffusion in porous cement-based materials, also including for mass exchange between solid constituents and ions dissolved in pore solution and, further, including electrical effects among the dissolved ions.

In every constitutive model, properties are divided into constitutive dependent and constitutive independent variables. In this model it will be assumed that the mol density concentration n_a, for all constituents, and the electric potential in solution φ are the constitutive independent properties. The constitutive dependent properties are: (i) the velocity $\dot{\mathbf{x}}_a$, (ii) the mass exchange rate among constituents $\hat{n}_a$, (iii) the electric displacement field vector $\mathbf{d}$ and (iv) the space charge density q. The constitutive dependent properties are assumed to be given as a function of the independent properties and their corresponding gradients in the following manner

$$(\dot{\mathbf{x}}_a, \hat{n}_a, \mathbf{d}, q) = f\left(n_{a=1,\ldots,\Re}, \text{grad}n_{a=1,\ldots,\Re}, \varphi, \text{grad}\varphi\right) \tag{11}$$

One important issue in constitutive modeling is to check that the material assumptions, as the one shown in expression (11), fulfill the requirements imposed by the second axiom of thermodynamics and the frame invariance. Such considerations do not, however, follow classical concepts when including electrical potential effects. One possibility is to treat the electric potential φ as a so-called hidden variable. The restrictions imposed by the second axiom of thermodynamics for the constitutive relations indicated in (11) will not be derived. This may be somewhat justified when thermal effects are excluded.

The $3\Re + 3$ unknown constitutive dependent and independent properties in this approach are

$$\begin{array}{ll} \Re \text{ number of :} & n_a(\mathbf{x}, t) \\ \Re \text{ number of :} & \dot{\mathbf{x}}_a(\mathbf{x}, t) \\ \Re \text{ number of :} & \hat{n}_a(\mathbf{x}, t) \\ & \mathbf{d}(\mathbf{x}, t) \\ & q(\mathbf{x}, t) \\ & \varphi(\mathbf{x}, t) \end{array} \tag{12}$$

One mass balance equation for each constituent is defined in equation (9). The conservation of mass during the mass exchange among constituents, i.e. (8), gives one extra equation related to balance of mass. That is, $\Re + 1$ equations are available for describing mass balance of the mixture. Further, one equation describes continuity for the density of the electrical current. The total number of physical balance laws is therefore $\Re + 2$. The difference

Table 1: Example of material constants for ions dissolved in water.

Substance	Diffusion coeff. (m^2/s)	Ionic mobility ($m^2/s/V$)	Dielectric coeff. (C/V)
Cl^-	$2.03 \cdot 10^{-9}$	$7.91 \cdot 10^{-8}$	-
OH^-	$5.30 \cdot 10^{-9}$	$20.64 \cdot 10^{-8}$	-
Na^+	$1.33 \cdot 10^{-9}$	$5.19 \cdot 10^{-8}$	-
K^+	$1.96 \cdot 10^{-9}$	$7.62 \cdot 10^{-8}$	-
Ca^{2+}	$0.79 \cdot 10^{-9}$	$6.17 \cdot 10^{-8}$	-
H_2O	-	-	$695.4 \cdot 10^{-12}$

between the number of unknown constitutive dependent and constitutive independent properties, and the number of physical balance laws, must be constitutive relations, which in this case is $2\Re + 1$ assumptions.

The assumption for the electric displacement field vector $\mathbf{d}$ is

$$\mathbf{d} = -\tilde{\varepsilon}\varepsilon_0 \text{grad}\varphi \tag{13}$$

where ε_0 (C/V) is the dielectrics coefficient or permittivity of vacuum, $\varepsilon_0 = 8.854 \cdot 10^{-12}$, and $\tilde{\varepsilon}$ (-) is the relative dielectric coefficient of a given substance that varies among different dielectrics. For water at 25^oC, $\tilde{\varepsilon}_w = 78.54$. The term $\text{grad}\varphi$ in equation (13) is the so-called electric field vector.

The charge density q is assumed to be given by the composition of positive and negative ions in solution in the following manner

$$q = F \sum_{a=1}^{\Re} n_a (\mathbf{x}, t) v_a \tag{14}$$

where $F = 96490\,(\text{C/mol})$ is a physical constant (Faraday's constant) describing the charge of one mol of an ion having a valence number, denoted v_a, equal to one. In a solution not in contact with narrow pore walls the relation (14) is more or less a definition of the charge density q. When including the charge character of narrow pore walls in contact with solution, the relation (14) may, in fact, be questioned, at least when treating each small representative volume as being smeared, containing averaged values of all the state variables including q. The mass exchange between ions in solution and ions included in solids is, however, in this paper assumed to be caused by chemical reactions rather than caused by creations of double layers

of positive and negative ions having their origin in a charged character of the solid pore walls.

The constitutive relation for the velocity for the $\Re$ ions 1, ..., $\Re$ is a Fick's first law type of equation with an extra term accounting for the effect of the electric field vector on the velocity. The following assumptions are used for the constituents:

$$\acute{\mathbf{x}}_a = -\frac{1}{n_a}\tilde{D}_a \text{grad} n_a - \tilde{A}_a v_a \text{grad}\varphi; \qquad a = 1, ..., \Re \tag{15}$$

where $\tilde{D}_a$ (m^2/s) and $\tilde{A}_a$ ($m^2/s/V$) are material constants. The tilde on top of D_a and A_a is used to stress that the values of D_a and A_a, given in Table 1, must be scaled to account for tortuosity effects in the pore system. Further, it should be noted that the diffusion coefficients D_a, presented in Table 1, are predicted values obtained by scaling the measured ionic mobilities A_a, e.g. see [3] and [4].

The material properties $\tilde{D}_a$ and $\tilde{A}_a$ are dependent on the shape and porosity of the pore system. It is, further, shown in [5] that pore size distribution and total porosity are changed during chloride penetration in concrete. This changes where measured with mercury porosimetry and X-ray diffraction. It was concluded that the change in the micro-structure is attributed to the formation of Friedel's salt.

The effect of the shape of the pore system on chloride diffusion in concrete has been investigated in [6] using a gas diffusion technique. The obtained tortuosity factor was in the range of 0.007-0.010 for a water to cement ratio 0.40 concrete, e.g. $\tilde{D}_a \approx 0.008 D_a$ for this case.

Theoretical consideration using a homogenization technique on the physical balance laws and constitutive relations has been adopted for chloride diffusion in concrete [7]. In this method a tortuosity factor is used to describe the influence of the shape of the pore system on the ion diffusion.

The degree of saturation of water, further, affects the diffusion of dissolved ions in pore space. This phenomenon has been studied theoretically using a lattice Boltzmann method in order to model phase separation of a binary mixture, including wetting effects [8]. At high saturations a good agreement between the semi-empirical Archie's second law was found. At low saturations, however, the law breaks down as percolation effects were shown to be important. That is, diffusion of dissolved ions in pore solution cannot occur when the liquid water phase is not connected.

The mol density exchange rates among the constituents will be assumed to be given as functions of the composition of the mixture in terms of the all $\Re$ individual mol densities, described in the following general manner

$$\hat{n}_b = f(n_1, n_2, ..., n_{\Re}) \qquad b = 1, ..., \Re - 1 \tag{16}$$

where it should be noted that only $\Re - 1$ mol density exchange rates are to be described due to the relation (8). Further, the equilibrium condition for the reactions must be included as a special case.

The $2\Re + 1$ assumptions needed to make the equation system closed is the $\Re$ number of assumptions of the velocities in (15), the $\Re - 1$ assumptions of the chemical reaction rates in (16) and the assumptions giving the electric displacement field $\mathbf{d}$ and the charge density q, i.e. equations (13) and (14), respectively.

The equilibrium conditions and kinetics of chloride binding are of central interest in this investigation. This binding is, however, dependent on the conditions of the components present in the solid and in the pore solution. When accounting for dielectric effects in the pore solution it is important not only to consider the chloride ions but also all other types of ions involved in chloride binding. A literature review of factors affecting chloride binding in cement-based materials can be found in [9]. Some of the main factors influencing binding of chlorides are the tricalcium aluminate content in cement, the water to binder ratio, the CaO/SiO_2 ratio, the pore solution alkalinity and cement replacement materials such as silica fume.

A general formulation for the aluminate phase can be described with the chemical formula $[CaO_2\,(Al,Fe)\,(OH)_6]^+Y^- \cdot mH_20$, where the brackets indicate the constitution of a positively charged layer unit. Molecular water is denoted by m. The excess positive charges are balanced by anions, denoted Y^-. These anions may typically be OH^- or externally supplied ions such as Cl^-, SO_4^{2-} and CO_3^-. In [10] the Friedel's salt $Ca_2Al(OH)_6Cl\text{-}2H_20$ and its relations with hydroxy AF_m are studied. The Friedel's salt is important since it is more stable than the hydroxy aluminate AF_m and due to AF_m serves as a 'sink' for chloride ions and thereby retards diffusion of chlorides. An equilibrium condition between Friedel's salt found in AF_m and pore fluid chloride concentration is established.

The kinetics of binding of chlorides is discussed in [11]. The time needed to reach equilibrium is observed to be in the range of 4 weeks, after which period the binding continues but is very slow. Measured relations, on different

concrete qualities, between total chloride content and free dissolved chloride in pore solution can be found in, e.g. [12], [13], [14], [15], [16], [17] and [18].

4 Reaction kinetics and chemical equilibrium conditions

Only three different chemical reactions will be assumed to take place in the system considered. The first reaction, shown by equation (17), describes binding of chloride ions present in pore solution by ion-exchange of $X\cdot(Ca(OH)_2)(s)$ to form $X\cdot(CaCl_2)(s)$. The symbol X is used as a general description for a more or less amorphous cement gel being interconnected with crystalline packages of calcium hydroxide. Further, this reaction is assumed to be irreversible, as

$$X\cdot(Ca(OH)_2)(s)+2Cl^-(aq) \longrightarrow 2OH^-(aq)+X\cdot(CaCl_2)(s) \qquad (17)$$

The second chemical reaction to be considered is dissolution of chloride ions from already formed calcium chloride being incorporated in the cement gel. This reaction is assumed to be irreversible:

$$X\cdot(CaCl_2)(s) \longrightarrow Ca^{2+}(aq)+2Cl^-(aq)+X(s) \qquad (18)$$

The third and last chemical reaction considered is dissolution of calcium hydroxide from the hydration products. The reaction is assumed to be reversible, as

$$X\cdot(Ca(OH)_2)(s) \rightleftarrows Ca^{2+}(aq)+2OH^-(aq)+X(s) \qquad (19)$$

For easier notation, the constituents will be denoted by subscripts ranging from 1 to 7 as; Cl^- (1), Na^+ (2), OH^- (3), Ca^{2+} (4), K^+ (5), $CaCl_2$ (6), and $Ca(OH)_2$ (7).

The equilibrium conditions in terms of the ion exchange equation (17) are the assumption

$$n_1^{eq} = (K + Zn_3)\, n_6; \qquad (20)$$

where K and Z are positive constants. Under the condition that the actual value of n_1 is equal to n_1^{eq} the ion exchange equation (17) is assumed not to be active. This condition assumes that at a certain mol density of bound $CaCl_2$ and at a certain mol density of dissolved OH^- in pore solution, a given

equilibrium mol density of dissolved Cl^- can be defined. Further, a high mol density of dissolved OH^- in pore solution gives a higher equilibrium value for the dissolved Cl^- than a low mol density of dissolved OH^- at a constant value of the mol density of bound $CaCl_2$. The influence of hydroxide concentration in the pore solution of hardened cement paste on chloride binding is investigated in [19].

The reaction described in equation (19) is assumed to have an equilibrium condition expressed by n_3^{eq}, given as

$$n_3^{eq} = W n_7 \tag{21}$$

When n_3^{eq} is equal to the actual value of n_3 the reaction (19) is assumed to be not active. That is, at a certain value of the mol density of solid $Ca(OH)_2$ a corresponding equilibrium value of the mol density of dissolved OH^- in pore solution exists.

The ion exchange reaction (17) is assumed to be active when displaced from its equilibrium condition as described in equation (19) on condition that $n_1^{eq} \leq n_1$. That is, if the actual value of the mol density of dissolved Cl^- in pore solution, i.e. n_1, is lower than the value of n_1^{eq} the solid product $X \cdot (CaCl_2)$ will be formed. The rate of formation or rate of consumption of Cl^- in this process will be assumed to be proportional to the 'distance' from equilibrium by using the constant R, as

$$\hat{n}_1^a = R\,(n_1^{eq} - n_1)\,; \quad \text{if} \quad n_1^{eq} \leq n_1 \tag{22}$$

where $\hat{n}_1^a$ denotes the production of Cl^- in pore solution due to reaction (17) taking place. Having the constant R as a positive number, $\hat{n}_1^a$ always becomes negative. The kinetic equation (22) describes the rate of mol density consumption of solid $X \cdot (Ca\,(OH)_2)(s)$ and dissolved Cl^- and the production of $X \cdot (CaCl_2)$ and dissolved OH^- in pore solution due to reaction (17) taking place. Due to the mol relation in equation (17) the following relation of rates can be established

$$\hat{n}_1^a = \tfrac{1}{2}\hat{n}_7^a = -\hat{n}_3^a = -\tfrac{1}{2}\hat{n}_6^a \tag{23}$$

The kinetic equation describing the rate of dissolution of chloride ions from already formed calcium chloride, being involved in the hydration products, is assumed to take place when $n_1^{eq} > n_1$, i.e. when the equilibration point for ion exchange according to equation (17) has been exceeded, at a rate proportional to the 'distance' from equilibrium as

$$\hat{n}_1^b = S\,(n_1^{eq} - n_1)\,; \quad \text{if} \quad n_1^{eq} > n_1 \tag{24}$$

where S is a positive number representing the rate constant for reaction (18) and where $\hat{n}_1^b$ denotes the mol density rate of formation of dissolved Cl^- in pore solution. The value $\hat{n}_1^b$ is always a positive number. Due to the mol relations in this reaction one can also establish the relations of rates as

$$\hat{n}_1^b = \tfrac{1}{2}\hat{n}_4^b = -\tfrac{1}{2}\hat{n}_6^b \tag{25}$$

The rate of the reversible reaction (19) is assumed to be constituted as

$$\hat{n}_3^c = Q\left(n_3^{eq} - n_3\right) \tag{26}$$

where $\hat{n}_3^c$ denotes the mole density rate of production of dissolved OH^-. Under conditions where $n_3^{eq} < n_3$ the value $\hat{n}_3^c$ becomes negative, i.e. binding of OH^- in solution onto the solid is assumed to be active. The mol density rates is in equation (19) related as

$$\hat{n}_3^c = \tfrac{1}{2}\hat{n}_4^c = -\tfrac{1}{2}\hat{n}_7^c \tag{27}$$

Finally, it is noted that the dissolved Na^+ and K^+ in pore solution is not involved in any chemical reactions, hence

$$\hat{n}_2 = 0; \quad \hat{n}_5 = 0 \tag{28}$$

It must be assured that no net production of mass occurs during the reactions according to the expression

$$\sum_{a=1}^{6} \hat{n}_a m_a = 0 \tag{29}$$

where $m_5 = (m_4 + 2m_1)$ and $m_6 = (m_4 + 2m_3)$ in which the different m-values represent the mass per mol of the different constituents.

Depending on the relations of the different mol density concentrations, either the reactions behind equation (17) and (19) or (18) and (19) will take place. By first considering the reactions in (17) and (19), which are valid under condition $n_1^{eq} \leq n_1$, the condition in (29) must be fulfilled. This is the case, which can be seen by summarizing all the reaction rates multiplied by their corresponding mol mass, as

$$\begin{aligned} 0 \;=\; & -R\left(n_1^{eq} - n_1\right) m_1 \\ & +R\left(n_1^{eq} - n_1\right) m_3 - Q\left(n_3^{eq} - n_3\right) m_3 \\ & -\tfrac{1}{2}Q\left(n_3^{eq} - n_3\right) m_4 \\ & +\tfrac{1}{2}R\left(n_1^{eq} - n_1\right)(m_4 + 2m_1) \\ & -\tfrac{1}{2}R\left(n_1^{eq} - n_1\right)(m_4 + 2m_3) + \tfrac{1}{2}Q\left(n_3^{eq} - n_3\right)(m_4 + 2m_3) \end{aligned} \tag{30}$$

The first to the last row in (30) represent the production of Cl^-, OH^-, Ca^{2+}, $CaCl_2$ and $Ca(OH)_2$, respectively.

Under conditions described by $n_1^{eq} > n_1$ the reactions shown in (18) and (19) are assumed to take place. The condition in (29) is also fulfilled for this case, since

$$\begin{aligned} 0 \;=\; & -S\left(n_1^{eq} - n_1\right) m_1 \\ & -Q\left(n_3^{eq} - n_3\right) m_3 \\ & -\tfrac{1}{2}Q\left(n_3^{eq} - n_3\right) m_4 - \tfrac{1}{2}S\left(n_1^{eq} - n_1\right) m_4 \\ & +\tfrac{1}{2}S\left(n_1^{eq} - n_1\right)\left(m_4 + 2m_1\right) \\ & +\tfrac{1}{2}Q\left(n_3^{eq} - n_3\right)\left(m_4 + 2m_3\right) \end{aligned} \tag{31}$$

where, again, the first to the last row in (31) represent the production of Cl^-, OH^-, Ca^{2+}, $CaCl_2$ and $Ca(OH)_2$, respectively.

5 Governing equations

This section will summarize the governing equations given from using the mass balance laws defined in the mixture theory together with the proposed constitutive relations and also by using the charge balance equation together with its corresponding constitutive assumptions.

The concentration fields $n_a\left(\mathbf{x}, t\right)$ for the 7 considered constituents, Cl^- (1), Na^+ (2), OH^- (3), Ca^{2+} (4), K^+ (5), $CaCl_2$ (6), and $Ca(OH)_2$ (7), are obtained by combining the mass balance equation (2) and the constitutive relation (15) describing the velocity and, further, by using the expressions for the chemical reaction rates described in section 4. It is also noted that the gradient of the electrostatic potential is involved to describe the velocity of the constituent. One extra equation is therefore necessary, to determine this potential. The differential equation determining the electrostatic potential φ becomes coupled to the diffusion equations and the diffusion equations are coupled to the electrostatic potential φ.

Since different chemical reactions are assumed to occur depending on whether $n_1^{eq} \leq n_1$ or $n_1^{eq} > n_1$, the equations shown will be related to one of these conditions and the other condition will be explained in the text.

The description of the chloride ions dissolved in the pore solution, denoted by the subscript 1, are under the condition $n_1^{eq} \leq n_1$ described as

$$\frac{\partial n_1}{\partial t} \;=\; \mathrm{div}\left(\tilde{D}_1 \mathrm{grad} n_1 + \tilde{A}_1 v_1 n_1 \mathrm{grad}\varphi\right) \tag{32}$$

$$+R\left(n_1^{eq}-n_1\right)$$

In cases where $n_1^{eq} > n_1$, the rate constant R is replaced by S. The equation (32) is obtained by combining equation (2) and the constitutive relations (15) and (22). When $n_1^{eq} > n_1$ the relation (22) is replaced by (24). The equilibrium value n_1^{eq} is given by the relation (20), which means that equation (32) is coupled to the equations determining the mol density of hydroxide, dissolved in pore solution, and solid calcium chloride.

Sodium ions, denoted by the subscript 2, appearing dissolved in the pore solution, are supposed not to take place in any chemical reactions. The governed equation for this constituent, therefore, is obtained by combining mass balance (2) and the constitutive relation (15) to obtain

$$\frac{\partial n_2}{\partial t} = \operatorname{div}\left(\tilde{D}_2 \operatorname{grad} n_2 + \tilde{A}_2 v_2 n_2 \operatorname{grad}\varphi\right) \tag{33}$$

The concentration field of hydroxide ions n_3, dissolved in the pore solution, are under the condition $n_1^{eq} \leq n_1$ described as

$$\begin{aligned}\frac{\partial n_3}{\partial t} &= \operatorname{div}\left(\tilde{D}_3 \operatorname{grad} n_3 + \tilde{A}_3 v_3 n_3 \operatorname{grad}\varphi\right) \\ &\quad -Q\left(n_3^{eq}-n_3\right) - R\left(n_1^{eq}-n_1\right)\end{aligned} \tag{34}$$

During conditions when $n_1^{eq} > n_1$ the material constant R is set to zero. Equation (34) is obtained by combining (2), (15), (22) and (26). When $n_1^{eq} > n_1$ equation (26) is not included. The equilibrium condition n_3^{eq} is given from equation (19) and n_1^{eq} from equation (20). That is, the differential equation (34) is coupled to the mol densities n_1, n_5 and n_6.

If the equilibrium condition for the chloride ions in pore solution is higher than the actual value, i.e. if $n_1^{eq} > n_1$, the equation governing the calcium ions in pore solution is obtained from the equations (2), (15), (24), (26), (25) and (27), as

$$\begin{aligned}\frac{\partial n_4}{\partial t} &= \operatorname{div}\left(\tilde{D}_4 \operatorname{grad} n_4 + \tilde{A}_4 v_4 n_4 \operatorname{grad}\varphi\right) \\ &\quad -\tfrac{1}{2}Q\left(n_3^{eq}-n_3\right) + \tfrac{1}{2}S\left(n_1^{eq}-n_1\right)\end{aligned} \tag{35}$$

When $n_1^{eq} \leq n_1$ the rate constant S is set to zero due to the reaction described in (24) not being active in this case.

Combining the mass balance (9) with the constitutive assumptions (15) and (28) gives the governed equation for the dissolved K^+ ions in pore solution as

$$\frac{\partial n_5}{\partial t} = \text{div}\left(\tilde{D}_5 \text{grad} n_5 + \tilde{A}_5 v_5 n_5 \text{grad}\varphi\right) \tag{36}$$

It will be explicitly assumed that the velocity for the solid $CaCl_2$ component is zero. That is, the differential equation describing the rate of change of the mol density of $CaCl_2$ is only due to chemical reactions. If the condition $n_1^{eq} \leq n_1$ holds, the mass balance (2), with inserted zero velocity, and with the chemical reaction rate assumption (22) together with the mol rate relation (23), gives the governed equation for the solid calcium chloride, as

$$\frac{\partial n_6}{\partial t} = -\tfrac{1}{2} R\left(n_1^{eq} - n_1\right) \tag{37}$$

When $n_1^{eq} > n_1$, R is replaced by S.

The solid calcium hydroxide constituent is also assumed to have zero velocity. During conditions when $n_1^{eq} \leq n_1$ the description of the solid calcium hydroxide is obtained by equation (2), with inserted zero velocity, and the description of the chemical reaction rate given from equations (24) and (26), together with the mol rate relations (23) and (27), as

$$\frac{\partial n_7}{\partial t} = \tfrac{1}{2} Q\left(n_3^{eq} - n_3\right) + \tfrac{1}{2} R\left(n_1^{eq} - n_1\right) \tag{38}$$

During situations when $n_1^{eq} > n_1$ the rate constant R is set to zero.

The last information needed is the equation describing the electrostatic potential φ, which is involved in all governing equations for the diffusing dissolved ions in the pore solution, i.e. the equations (32), (33), (34) and (35). By using the static continuity equation for the charge (10) together with the constitutive relations for the electric displacement field vector $\mathbf{d}$ (13) and the charge density q (14) the governing equation for the electrostatic potential becomes

$$-\text{div}\left(\tilde{\varepsilon}\varepsilon_0 \text{grad}\varphi\right) = F \sum_{a=1}^{5} n_a\left(\mathbf{x}, t\right) v_a, \tag{39}$$

When using this method to calculate the 7 concentration fields $n_a\left(\mathbf{x}, t\right)$ the eletroneutrality $\phi\left(\mathbf{x}, t\right)$ will not be satisfied, i.e.

$$\phi\left(\mathbf{x}, t\right) = \sum_{a=1}^{5} n_a\left(\mathbf{x}, t\right) v_a \neq 0. \tag{40}$$

However, due to the time scale in the problem the potential $\phi(\mathbf{x}, t)$, as defined above, will be very close to the value zero.

Excluding the physical constant F, the model includes in total 17 material constants. The description of the velocity of the dissolved ions involves 5 diffusion constants and 5 ionic mobility constants, the description leading to a determination of the electrostatic potential involves one constant, i.e. the property $\tilde{\varepsilon}\varepsilon_0$, the description of the chemical equilibrium conditions involves 3 constants, i.e. K, Z and W, and the description of the kinetics of the considered chemical reactions involves 3 rate constants, i.e. R, S and Q.

6 Solution strategy

In order to check the reasonableness of the assumptions leading to the governing equations in section 5, a test example will be solved by giving numbers to the 17 defined material constants. The result from such a computation can be compared to general observations obtained from experiments. The 7 governed differential equations presented in section 5 are coupled and non-linear. A numerical method is therefore needed. Here the finite element method will be used. This concept can be studied in, e.g. [20], [21], [22] and [23].

The total equation system will be brought to the form

$$\mathbf{C}^{\mathrm{t}}\dot{\mathbf{a}}^{\mathrm{t}} + \mathbf{K}^{\mathrm{t}}\mathbf{a}^{\mathrm{t}} + \mathbf{f}^{\mathrm{t}} = \mathbf{0}, \tag{41}$$

where $\mathbf{C}^{\mathrm{t}}$, $\mathbf{K}^{\mathrm{t}}$ and $\mathbf{f}^{\mathrm{t}}$ are the total damping matrix, stiffness matrix and load/boundary vector, respectively. At a certain time level, the total concentration vector $\mathbf{a}^{\mathrm{t}}$ contains all spatial distributions of all 7 different constituents and the electrostatic potential. The property $\dot{\mathbf{a}}^{\mathrm{t}}$ contains the corresponding time derivatives.

A finite time increment Δt will be considered, which is related to the time levels t_i and t_{i+1} as $t_{i+1} = t_i + \Delta t$, in order to obtain so-called recurrence relations. A time integration parameter Θ is introduced where $\Theta = 0$ is a truly explicit scheme, $\Theta = 1$ is a truly implicit scheme, $\Theta = 0.5$ is the Crank-Nicholson scheme and $\Theta = 0.878$ is the Liniger scheme in which Θ is chosen to minimize the whole domain error. Values of Θ greater than or equal to 0.5 are shown to be unconditionally stable for equation systems which are symmetric and positive definite. The time derivative is formed according to the one step scheme, i.e. $\dot{\mathbf{a}}^{\mathrm{t}} = \left(\mathbf{a}^{\mathrm{t}}_{i+1} - \mathbf{a}^{\mathrm{t}}_{i}\right)/\Delta t$, where $\mathbf{a}^{\mathrm{t}}_{i}$ is given at time level

t and $\mathbf{a}^{\mathrm{t}}_{i+1}$ at time level $t+\Delta t$. The concentration vector $\mathbf{a}^{\mathrm{t}}$ is weighted with the time integration parameter Θ as: $\mathbf{a}^{\mathrm{t}} = \mathbf{a}^{\mathrm{t}}_i + \Theta\left(\mathbf{a}^{\mathrm{t}}_{i+1} - \mathbf{a}^{\mathrm{t}}_i\right)$. Hence, (41) can be brought to the form

$$\begin{aligned} \mathbf{0} \;=\; & \frac{\mathbf{C}^{\mathrm{t}}\left(\mathbf{a}^{\mathrm{t}}_{i+1} - \mathbf{a}^{\mathrm{t}}_i\right)}{\Delta t} + \mathbf{K}^{\mathrm{t}}\left(\mathbf{a}^{\mathrm{t}}_i + \Theta\left(\mathbf{a}^{\mathrm{t}}_{i+1} - \mathbf{a}^{\mathrm{t}}_i\right)\right) \\ & + \mathbf{f}^{\mathrm{t}}_i + \Theta\left(\mathbf{f}^{\mathrm{t}}_{i+1} - \mathbf{f}^{\mathrm{t}}_i\right). \end{aligned} \tag{42}$$

where the load/boundary vector $\mathbf{f}^{\mathrm{t}}$ is weighted as $\mathbf{f}^{\mathrm{t}} = \mathbf{f}^{\mathrm{t}}_i + \Theta\left(\mathbf{f}^{\mathrm{t}}_{i+1} - \mathbf{f}^{\mathrm{t}}_i\right)$. The equation (42) is used to solve the unknown vector $\mathbf{a}^{\mathrm{t}}_{i+1}$.

The matrix associated with the time derivative of the state variables is $\mathbf{C}^{\mathrm{t}}$, formed by assembling the damping matrixes for the individual diffusion equations as block matrixes, is established as

$$\mathbf{C}^{\mathrm{t}} = \begin{bmatrix} \mathbf{C}_1 & \mathbf{0} & \mathbf{0} & \mathbf{0} & \mathbf{0} & \mathbf{0} & \mathbf{0} & \mathbf{0} \\ \mathbf{0} & \mathbf{C}_2 & \mathbf{0} & \mathbf{0} & \mathbf{0} & \mathbf{0} & \mathbf{0} & \mathbf{0} \\ \mathbf{0} & \mathbf{0} & \mathbf{C}_3 & \mathbf{0} & \mathbf{0} & \mathbf{0} & \mathbf{0} & \mathbf{0} \\ \mathbf{0} & \mathbf{0} & \mathbf{0} & \mathbf{C}_4 & \mathbf{0} & \mathbf{0} & \mathbf{0} & \mathbf{0} \\ \mathbf{0} & \mathbf{0} & \mathbf{0} & \mathbf{0} & \mathbf{C}_5 & \mathbf{0} & \mathbf{0} & \mathbf{0} \\ \mathbf{0} & \mathbf{0} & \mathbf{0} & \mathbf{0} & \mathbf{0} & \mathbf{0} & \mathbf{0} & \mathbf{0} \\ \mathbf{0} & \mathbf{0} & \mathbf{0} & \mathbf{0} & \mathbf{0} & \mathbf{0} & \mathbf{C}_6 & \mathbf{0} \\ \mathbf{0} & \mathbf{0} & \mathbf{0} & \mathbf{0} & \mathbf{0} & \mathbf{0} & \mathbf{0} & \mathbf{C}_7 \end{bmatrix} \tag{43}$$

The time derivative of the total concentration vector $\mathbf{a}^{\mathrm{t}}$ is, further, arranged as

$$\dot{\mathbf{a}}^{\mathrm{t}} = \begin{bmatrix} \dot{\mathbf{a}}_1 \\ \dot{\mathbf{a}}_2 \\ \dot{\mathbf{a}}_3 \\ \dot{\mathbf{a}}_4 \\ \dot{\mathbf{a}}_5 \\ \mathbf{0} \\ \dot{\mathbf{a}}_6 \\ \dot{\mathbf{a}}_7 \end{bmatrix} \tag{44}$$

where the subscripts, ranging from 1 to 7, denote the constituents, Cl^- (1), Na^+ (2), OH^- (3), Ca^{2+} (4), K^+ (5), $CaCl_2$ (6), and $Ca(OH)_2$ (7).

The chemical reactions will be involved in the total stiffness $\mathbf{K}^{\mathrm{t}}$, on con-

dition that $n_1^{eq} \leq n_1$, as

$$\mathbf{K}_a^t = \begin{bmatrix} \mathbf{K}_1 + \mathbf{R}_1^a & \mathbf{0} & \mathbf{0} & \mathbf{0} & \mathbf{0} & \mathbf{V}_{\varphi 1}(\mathbf{a}_1) & -\mathbf{R}_6^a(\mathbf{a}_3) & \mathbf{0} \\ \mathbf{0} & \mathbf{K}_2 & \mathbf{0} & \mathbf{0} & \mathbf{0} & \mathbf{V}_{\varphi 2}(\mathbf{a}_2) & \mathbf{0} & \mathbf{0} \\ -\mathbf{R}_1^a & \mathbf{0} & \mathbf{K}_3 - \mathbf{R}_3 & \mathbf{0} & \mathbf{0} & \mathbf{V}_{\varphi 3}(\mathbf{a}_3) & \mathbf{R}_6^a(\mathbf{a}_3) & \mathbf{R}_7 \\ \mathbf{0} & \mathbf{0} & -\frac{1}{2}\mathbf{R}_3 & \mathbf{K}_4 & \mathbf{0} & \mathbf{V}_{\varphi 4}(\mathbf{a}_4) & \mathbf{0} & \frac{1}{2}\mathbf{R}_7 \\ \mathbf{0} & \mathbf{0} & \mathbf{0} & \mathbf{0} & \mathbf{K}_5 & \mathbf{V}_{\varphi 5}(\mathbf{a}_5) & \mathbf{0} & \mathbf{0} \\ \mathbf{E}_{\varphi 1} & \mathbf{E}_{\varphi 2} & \mathbf{E}_{\varphi 3} & \mathbf{E}_{\varphi 4} & \mathbf{E}_{\varphi 5} & \mathbf{K}_\varphi & \mathbf{0} & \mathbf{0} \\ -\frac{1}{2}\mathbf{R}_1^a & \mathbf{0} & \mathbf{0} & \mathbf{0} & \mathbf{0} & \mathbf{0} & \frac{1}{2}\mathbf{R}_6^a(\mathbf{a}_3) & \mathbf{0} \\ \frac{1}{2}\mathbf{R}_1^a & \mathbf{0} & \frac{1}{2}\mathbf{R}_3 & \mathbf{0} & \mathbf{0} & \mathbf{0} & -\frac{1}{2}\mathbf{R}_6^a(\mathbf{a}_3) & -\frac{1}{2}\mathbf{R}_7 \end{bmatrix} \tag{45}$$

where the stiffness matrix for the concentration gradient dependent diffusion is formed as $\mathbf{K}_a = \int_V \mathbf{B}^{\mathrm{T}} \tilde{D}_a \mathbf{B} dV$, where $\mathbf{B}(\mathbf{x})$ is defined as the gradient of the shape function, i.e. $\mathbf{B}(\mathbf{x}) = \boldsymbol{\nabla}\mathbf{N}(\mathbf{x})$. The stiffness matrix for the electrical displacement field is formed as $\mathbf{K}_\varphi = \int_V \mathbf{B}^{\mathrm{T}} \tilde{\varepsilon}\varepsilon_0 \mathbf{B} dV$. The stiffness matrix for the part of the mass flow which is dependent on the gradient of the electrostatic potential φ is formed as $\mathbf{V}_{\varphi a}(\mathbf{a}_a) = \int_V \mathbf{B}^{\mathrm{T}} \tilde{A}_a v_a(\tilde{a}_a) \mathbf{B} dV$ where the parameter $\tilde{a}_a$ is a smeared element value of the nodal concentrations of the constituent a. The term related to the charge density q is $\mathbf{E}_{\varphi a} = \int_V \mathbf{N}^{\mathrm{T}} F v_a \mathbf{N} dV$.

The chemical reactions, on condition that $n_1^{eq} \leq n_1$, are formed as $\mathbf{R}_1^a = \int_V \mathbf{N}^{\mathrm{T}} R \mathbf{N} dV$, $\mathbf{R}_3 = \int_V \mathbf{N}^{\mathrm{T}} Q \mathbf{N} dV$, $\mathbf{R}_5^a = \int_V \mathbf{N}^{\mathrm{T}} R(K + Z(\tilde{a}_3)) \mathbf{N} dV$ and $\mathbf{R}_6 = \int_V \mathbf{N}^{\mathrm{T}} Q W \mathbf{N} dV$.

On condition that $n_1^{eq} > n_1$, the total stiffness can be formulated as

$$\mathbf{K}_b^t = \begin{bmatrix} \mathbf{K}_1 + \mathbf{R}_1^b & \mathbf{0} & \mathbf{0} & \mathbf{0} & \mathbf{0} & \mathbf{V}_{\varphi 1}(\mathbf{a}_1) & -\mathbf{R}_6^b(\mathbf{a}_3) & \mathbf{0} \\ \mathbf{0} & \mathbf{K}_2 & \mathbf{0} & \mathbf{0} & \mathbf{0} & \mathbf{V}_{\varphi 2}(\mathbf{a}_2) & \mathbf{0} & \mathbf{0} \\ \mathbf{0} & \mathbf{0} & \mathbf{K}_3 - \mathbf{R}_3 & \mathbf{0} & \mathbf{0} & \mathbf{V}_{\varphi 3}(\mathbf{a}_3) & \mathbf{0} & \mathbf{R}_7 \\ \frac{1}{2}\mathbf{R}_1^b & \mathbf{0} & -\frac{1}{2}\mathbf{R}_3 & \mathbf{K}_4 & \mathbf{0} & \mathbf{V}_{\varphi 4}(\mathbf{a}_4) & -\frac{1}{2}\mathbf{R}_6^b(\mathbf{a}_3) & \frac{1}{2}\mathbf{R}_7 \\ \mathbf{0} & \mathbf{0} & \mathbf{0} & \mathbf{0} & \mathbf{K}_5 & \mathbf{V}_{\varphi 5}(\mathbf{a}_5) & \mathbf{0} & \mathbf{0} \\ \mathbf{E}_{\varphi 1} & \mathbf{E}_{\varphi 2} & \mathbf{E}_{\varphi 3} & \mathbf{E}_{\varphi 4} & \mathbf{E}_{\varphi 5} & \mathbf{K}_\varphi & \mathbf{0} & \mathbf{0} \\ -\frac{1}{2}\mathbf{R}_1^b & \mathbf{0} & \mathbf{0} & \mathbf{0} & \mathbf{0} & \mathbf{0} & \frac{1}{2}\mathbf{R}_6^b(\mathbf{a}_3) & \mathbf{0} \\ \mathbf{0} & \mathbf{0} & \frac{1}{2}\mathbf{R}_3 & \mathbf{0} & \mathbf{0} & \mathbf{0} & \mathbf{0} & -\frac{1}{2}\mathbf{R}_7 \end{bmatrix} \tag{46}$$

where the chemical reactions differ in $\mathbf{R}_1^b$ and $\mathbf{R}_5^b$ compared to $\mathbf{R}_1^a$ and $\mathbf{R}_5^a$ in (45). The properties $\mathbf{R}_1^b$ and $\mathbf{R}_5^b$, associated with the reaction (17), are given as $\mathbf{R}_1^b = \int_V \mathbf{N}^{\mathrm{T}} S \mathbf{N} dV$ and $\mathbf{R}_5^a = \int_V \mathbf{N}^{\mathrm{T}} S(K + Z(\tilde{a}_3)) \mathbf{N} dV$.

The total load/boundary vector is expressed as

$$\hat{\mathbf{f}}^{\mathrm{t}} = \begin{bmatrix} \mathbf{f}_1 \\ \mathbf{f}_2 \\ \mathbf{f}_3 \\ \mathbf{f}_4 \\ \mathbf{f}_5 \\ \mathbf{f}_\varphi \\ \mathbf{f}_6 \\ \mathbf{f}_7 \end{bmatrix}. \tag{47}$$

The load/boundary vector for the diffusion equations is in general terms written as $\mathbf{f}_a = -\int_{S_h} \mathbf{N}^{\mathrm{T}} h_a dS - \int_{S_{n=g}} \mathbf{N}^{\mathrm{T}} q_a dS$, where h_a is a prescribed value of the normal flow of ions through the boundary surface S_h and q_a is the value of the flow through the boundary surface $S_{n=g}$ on which the concentration n_a has been prescribed. The values of q_a can be calculated whenever the concentration n_a is prescribed at the same material point.

The equation system (42) is solved directly, i.e. without using any staggered method, which means that all concentration fields for the different constituents and for the electric potential in the domain are evaluated in one step only, at each time level. No special methods are used to tackle the non-linearities by using iterations within time steps. A simple Euler forward approach is adopted in which the non-linear parameters are adjusted before proceeding to the next time step. The error made in this approach was tested, simply by checking the effect of decreasing the time step length. A time step length was chosen so that a further decrease did not change the solution.

In order to obtain stable solutions an implicit time integration was used. This type of time integration method is, indeed, in conflict with the Euler forward method used for tackling the non-linearities. The errors introduced are, however, estimated to be rather small.

7 Experimental procedure

In [24] a whole series of experiments on chloride penetration into concrete are presented. Different types of concrete qualities and curing conditions before exposure to a 3 wt.% sodium chloride solution were tested. Here the tests on a Swedish sulfate-resistent Portland cement (SRPC) with 5% of cement

Table 2: Mix proportions, water to binder ratio 0.55.

	Weight (kg/m^3)	Weight in the mix (kg)	Moisture (kg)
Cement (SRPC)	323	7.106	-
Silica fume	17	0.374	-
Aggregate 0-8 mm	966	21.252	0.0808
Aggregate 8-12 mm	857	18.85	-
Water	187	4.0332	-
Plasticizer	-	-	-

weight being replaced by silica fume will be described. The samples were membrane hardened one day after casting and then dried for two weeks in room climate followed by storage in tap water for one week. After this pre-curing condition samples were submerged in the chloride solution for 119 days, [24].

Another frequently used method leading to the determination of the effective chloride diffusion constant in concrete is an accelerated technique using an external applied electrical field, e.g. see [25] and [26]. Short-term tests on cement paste have also been presented using chloride exposure times between half an hour up to three hours without using external applied electrical fields. In this method 0.1 mm layers were removed by grinding. The concrete powder was analyzed for chloride content using a potentiometric titration apparatus [27].

In order to examine the chloride ingress, three different water to binder ratio concretes were produced. Their mix proportions are presented in Table 2-4. The typical composition of the cement and silica fume used is presented in Table 5.

The concretes were cast in plastic (PVC) cylinders with inner diameter 100 mm and with a length of 180 mm. Samples where vibrated on a table for approximately one minute directly after molding. Samples were then sealed with plastic foil to prevent moisture exchange with the surroundings. One day after casting, samples from each concrete quality were cut into two discs with a thickness of 25 mm and one disc with thickness 60 mm. The plastic mold and sealing were then removed from the 25 mm thick specimens. The 60 mm thick specimens were tightened with silicon rubber in the joint between the concrete and the plastic cylinder. Thereafter the two 25 mm and

Table 3: Mix proportions, water to binder ratio 0.40.

	Weight (kg/m^3)	Weight in the mix (kg)	Moisture (kg)
Cement (SRPC)	399	8.778	-
Silica fume	21	0.462	-
Aggregate 0-8 mm	898	19.756	0.0790
Aggregate 8-12 mm	898	19.756	-
Water	168	3.5269	-
Plasticizer	6.3	0.138	0.0901

the 60 mm thick specimens, from each concrete quality, were stored in room climate for two weeks, allowing for drying and some additional hydration. After that, one of the 25 mm samples and the 60 mm thick sample were stored one week in a water bath. The dry 25 mm samples were used to examine the capillary suction by regularly measuring the weight gain as a function of time with the specimen put in contact with a free water surface. The best fit of the mass gain as a function of the square root of time was obtained and found to be: $7.83 \cdot 10^{-3}$, $11.4 \cdot 10^{-3}$ and $107.3 \cdot 10^{-3}$ ($kg/m^2/\sqrt{t}$), for the water to binder ratios 0.35, 0.40 and 0.55, respectively. The maximum specimen volume occupied by water due to capillary suction, at equilibrium, here referred to as the 'active porosity', for the three concrete qualities are given in Table 6. The time needed to reach equilibrium was approximately 1, 10 and 25 days for the water to binder ratios 0.55, 0.40 and 0.35, respectively. Table 6 only gives water that was sucked in during test. The total water content is higher due to the fact that the concrete was not totally dried when the test started. The calculated capillary porosities using the formula: $P_{cap} = C/1000\,(w/b - 0.19\alpha)$, where C is the mass density concentration of cement in mix, w/b is the water to binder ratio and α is the degree of hydration, are shown in Table 6.

After the preparation of samples, as described above, the 25 mm samples were taken from the water bath and the degree of hydration was measured. The 60 mm samples were taken from the water bath and were placed in a container with approximately 200 liters of 3 wt.% sodium chloride solution.

The degree of hydration was measured by first heating a finely crushed representative part of the samples to 105 °C for 40 days, which was the time needed for stabilization of the weight. After that, the samples were stored in

Table 4: Mix proportions, water to binder ratio 0.35.

	Weight (kg/m^3)	Weight in the mix (kg)	Moisture (kg)
Cement (SRPC)	427.5	9.405	-
Silica fume	22.5	0.495	-
Aggregate 0-8 mm	858	18.876	0.0717
Aggregate 8-12 mm	929	20.438	-
Water	157.5	3.2646	-
Plasticizer	9.0	0.198	0.1287

Table 5: Typical composition of the cement and pozzolan used.

Component	Composition SRPC (Percent of total)	Composition Silica (Percent of total)
Ca0	63.8	0.4
SiO_2	22.8	94.2 (amorph.)
Al_2O_3	3.48	0.62
Fe_2O_3	4.74	0.95
MgO	0.80	0.65
SO_3	1.88	0.33
K_2O	0.55	0.5
Na_2O	0.06	0.2
Ignition loss	0.72	1.8

an exsiccator with dry air at room temperature for approximately one day and then they were weighed. The samples were then heated to 1050 °C for approximately 16 hours, in order to remove the chemically bound water, and then again placed in the exsiccator. Finally, the samples were weighed after cooling to room temperature. The loss on ignition of the cement, pozzolan and gravel used was measured separately after heating to 1050 °C. The loss on ignition was 0.689 wt.% for cement, 0.712 wt.% for the sand 0-8 mm, 0.250 wt.% for for the gravel 8-16 mm, and 1.304 wt.% for silica fume.

Table 6: Amount of water absorbed during the capillary suction experiments expressed in terms of active porosity.

Concrete (w/b)	Active porosity (m^3/m^3 of concrete)	Calc. capillary porosity (m^3/m^3 of concrete)
0.35	0.0562	0.0563
0.40	0.0788	0.0740
0.55	0.1073	0.1046

The hydration α was evaluated using the following formula

$$\alpha = \frac{W_n}{C} = \frac{W_{105}\left(1 - \left(\frac{\mu_a + \Gamma\mu_c}{1+\Gamma}\right)\right) - W_{1050}}{W_{1050} - (1-\mu_a)\left(\frac{\Gamma}{1+\Gamma}\right)W_{105}} \tag{48}$$

where W_n is the chemically bound water (kg), C is the weight of cement (kg), W_{105} is the weight after heating to 105 ^{o}C (kg), W_{1050} is the weight after heating to 1050 ^{o}C (kg), Γ is the ratio of gravel weight to cement weight, aggregate/cement (kg/kg), μ_a is the loss on ignition for gravel and pozzolans (kg/kg), μ_c is the loss on ignition for cement (kg/kg).

The degree of hydration α for the three tested concrete qualities, using equation (48), was 0.56 (w/b 0.35), 0.55 (w/b 0.4) and 0.58 (w/b 0.55). It should be observed that the use of equation (48) may be questioned, when adding silica fume to the cement, since the calcium hydroxide and silica fume is believed to form so-called polymerization chains. In this reaction water is formed which not is accounted for in the equation (48).

The 60 mm samples for evaluation of chloride penetration were stored in 3 wt. % sodium chloride solution for 119 days at room temperature. The sodium chloride solution in the container was replaced twice during the exposure to prevent effects caused by leaching of ions from concrete and consumption of chlorides from solutions into concrete. After 119 days the samples were removed from the container for chloride profile analyses.

The sample was placed in a grinding device which enables removal of layers from the exposed concrete surface with a precision in the order of 0.1 mm in depth. Typically 1 mm thick layers were removed and the concrete powder from each layer was collected in small plastic bags which were sealed and marked. The depth from the exposed surface to the depth at which the concrete dust was collected, was measured with a slide-calliper at several locations and a mean value of these values was used.

Table 7: Measured chloride profile in terms of total chloride (bound + free). Water to binder ratio 0.55. The sample was unidirectionally dried in room climate for two weeks and re-wetted for one week in tap water before being exposed to a 3 weight percent sodium chloride solution for 119 days.

Depth (mm)	U (mV)	Total Cl^- (wt % of concrete)
0.0-1.0	22.8	0.163
1.0-2.0	19.4	0.188
2.0-2.9	20.6	0.179
2.9-4.1	20.9	0.177
4.1-5.1	22.4	0.166
6.6-8.5	32.1	0.110
10.7-12.3	46.9	0.059
16.1-17.5	78.4	0.015
21.9-23.7	118.6	0.003
27.0-29.6	120.9	0.003

The analysis method used for detecting chloride was the RCT-method (Rapid Chloride Test) [28]. 1.5 ± 0.005 gram of the concrete dust was collected from each layer and was placed in a vial containing 10 ml of an extraction liquid. The containers were sealed and shaken for approximately 10 minutes. Chloride ions dissolved in this solution were measured with an ion-selective electrode giving a number in terms of millivolts. The electrode was calibrated against four reference solutions with different chloride content. Before evaluating a chloride profile the electrode was calibrated. The best fit obtained by two independent calibration procedures on well-defined reference solutions gave the following relations, $C_{Cl} = 0.4270 \exp(-0.04154U)$ and $C_{Cl} = 0.4283 \exp(-0.04238U)$, where C_{Cl} is the wt.% chloride of concrete and U is the values measured by the electrode in mV. The first relation is used for the data shown in Table 9, and the second relation is used for the data shown in Table 7 and 9. As a verification of the performance of the ion-selective electrode a titration, using a silver anode, was performed on nine different samples. The results from this instrument (CIBA-CORNING Chloride Analyzer) were compared with the ion electrode measurements described above, i.e. the RCT-method, and it was found that the titration measurements gave systematically higher values compared to the ion elec-

Table 8: Measured chloride profile in terms of total chloride (bound + free). Water to binder ratio 0.40. The sample was unidirectionally dried in room climate for two weeks and re-wetted for one week in tap water before being exposed to a 3 weight percent sodium chloride solution for 119 days.

Depth (mm)	U (mV)	Total Cl^- (wt % of concrete)
0.0-0.9	19.0	0.191
0.9-1.8	14.1	0.236
1.8-2.6	13.9	0.238
2.6-4.0	15.2	0.225
4.0-6.0	19.8	0.185
6.0-7.5	27.6	0.133
10.1-11.0	60.7	0.003
15.1-16.5	116.6	0.003
22.1-24.3	120.9	0.003
28.9-30.2	121.1	0.003

trode measurements. The lowest ratio of titration to ion electrode results was 1.00 and the highest value 1.17. The mean value was 1.09 for the nine comparisons performed.

The measured chloride content as a function of the depth from the exposed surface is presented in Table 7-9.

The compressive strength of cubes was measured at 7days from casting giving the results 77 MPa (w/b 0.35), 66 MPa (w/b 0.4) and 39 MPa (w/b 0.55).

Experimental data of the composition of the pore solution, for a 5-month-old concrete, stored in water, produced with the cement described in Table 5 with a water to binder ratio of 0.4 with 5% silica, are presented in Table 10. These experiments were performed by EUROC RESEARCH AB. The water in concrete was drained by applying pressure to the sample. The potassium and sodium ions were detected with IPC-analyses and the hydroxide ions using titration.

Table 9: Measured chloride profile in terms of total chloride (bound + free). Water to binder ratio 0.35. The sample was unidirectionally dried in room climate for two weeks and re-wetted for one week in tap water before being exposed to a 3 weight percent sodium chloride solution for 119 days.

Depth (mm)	U (mV)	Total Cl^- (wt % of concrete)
0.0-1.0	15.7	0.222
1.0-2.0	12.1	0.258
2.0-2.9	12.6	0.253
2.9-5.0	18.4	0.199
5.0-5.9	30.5	0.120
8.8-9.8	68.1	0.025
12.1-13.6	103.2	0.006
17.7-19.8	125.3	0.002
26.6-29.1	126.5	0.002

Table 10: Pore extraction data for a 5-month-old concrete with water to binder ratio 0.40. The concrete was stored in water during the whole time. Cement as described in Table 5, with silica (5 mass percent of cement weight)

Material	K^+ (mmol/l)	Na^+ (mmol/l)	OH^- (mmol/l)	(Error) -
w/b 0.40	255	34	286	3

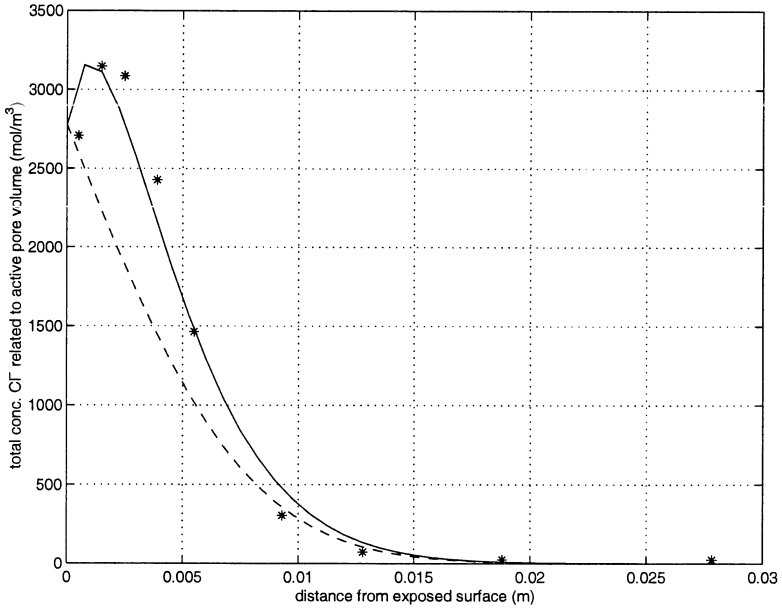

Figure 1: *Results for the SRPC concrete, with 5 wt. % silica fume replacing cement, having water to binder ratio 0.35. Total concentration of chloride ions (bound + free) in relation to the active pore volume after 119 days of exposure to a 3 wt. % sodium chloride solution. The stars represent measured values. The dashed line is the result from the simulation when not taking into account dielectric effects, and the solid line is the case when dielectric effects are considered.*

8 Test results compared with calculations

A simulation of the chloride transport in a porous cement-based material being subjected to a sodium chloride solution is performed. The equations shown in section 5 will be solved using the finite element scheme outlined in section 6. The material constants will be chosen so as to get the best fit with experimental data given in section 7. The initial conditions in terms of mol concentrations of ions in pore solution are for K^+, Na^+, OH^- and Ca^+ set to 255, 31, 306 and 10 (mol/m^3), values which are in the range corresponding to the measured values given in Table 10. The outer concentration of sodium chloride is set to 510 mol/m^3, which corresponds to the conditions in the experiments to which the test results are to be compared.

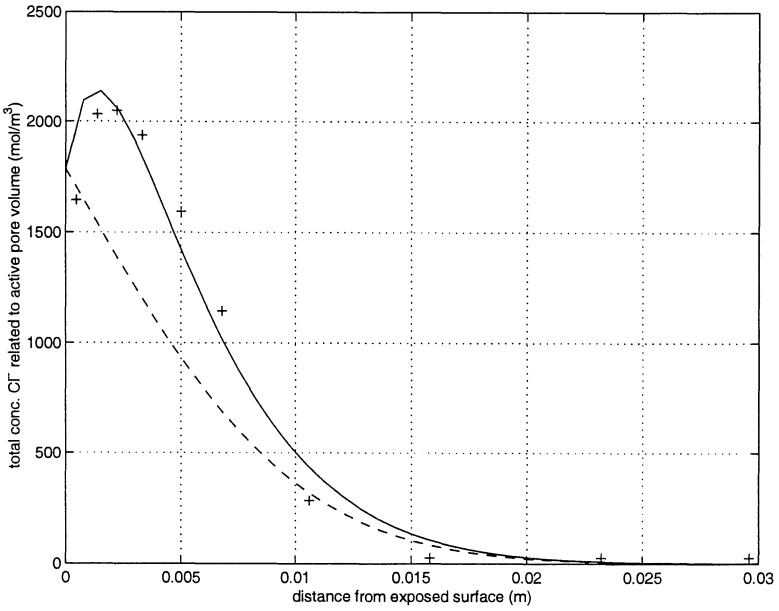

Figure 2: *Results for the SRPC concrete, with 5 wt. % silica fume replacing cement, having water to binder ratio 0.40. Total concentration of chloride ions (bound + free) in relation to the active pore volume after 119 days of exposure to a 3 wt. % sodium chloride solution. The stars represent measured values. The dashed line is the result from the simulation when not taking into account dielectric effects, and the solid line is the case when dielectric effects are considered.*

The values of the diffusion coefficients and ion mobility coefficients for the ions in pore solution are based on the values presented in Table 1. These values are scaled in order to account for the decreased diffusion due to tortuosity in the pore system. The tortuosity factor is assumed constant during exposure, i.e. the influence of continued hydration of cement and the chemical reactions, described in section 4, on the micro-structure are ignored. That is, the obtained value of tortuosity, for a certain concrete quality, should be seen as an averaged property over the entire test time.

The equilibrium conditions for the chemical reactions described in section 4 are given by the constants K (-), Z (m^3/mol) and W (-). Further, the kinetics of the considered reactions are described by the constants R (1/s), S (1/s) and Q (1/s). Due to a constant outer exposure of chloride ions in

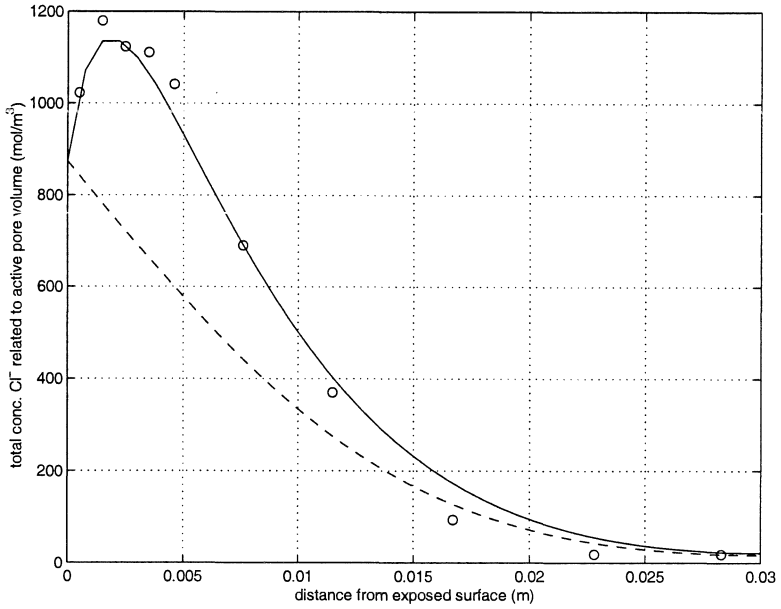

Figure 3: *Results for the SRPC concrete, with 5 wt. % silica fume replacing cement, having water to binder ratio 0.55. Total concentration of chloride ions (bound + free) in relation to the active pore volume after 119 days of exposure to a 3 wt. % sodium chloride solution. The stars represent measured values. The dashed line is the result from the simulation when not taking into account dielectric effects, and the solid line is the case when dielectric effects are considered.*

the experiments used, the dissolution of chloride ions from already formed solid calcium chloride is ignored by not including reaction (18), which means that the material constant S describing the rate of dissolution of chlorides becomes equal to zero. The influence of chloride binding on the hydroxide concentration in the pore solution (i.e. on the pH-value) is also ignored by setting the material constant Z to zero, see equation (20).

The coefficient of permittivity $\tilde{\varepsilon}\varepsilon_0$ is set to $6.95 \cdot 10^{-10}$ (C/V), which is the value valid for bulk water at 25°C. No scaling of this coefficient is performed, since the determination of the electrostatic field, which needs the information of the value of the permittivity $\tilde{\varepsilon}\varepsilon_0$, is related to ions dissolved in pore solution only.

The one-dimensional domain considered is 60 mm and exposed at both

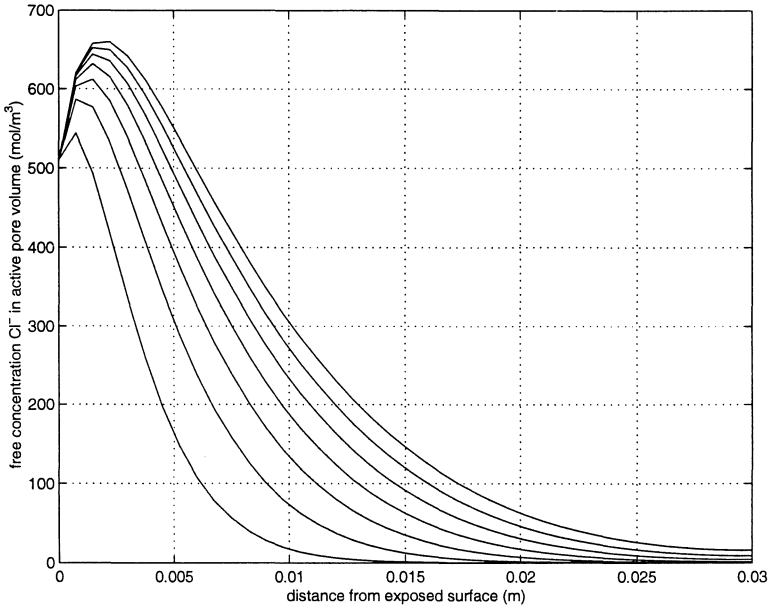

Figure 4: *Calculated free concentration of dissolved chloride ions in active pore volume for the SRPC concrete with 5% silica fume, w/b 0.55. The profiles represent exposure up to 119 days. The time step length between profiles shown is 17 days (profiles develop from left to right). The active water filled porosity is measured as 0.107 (m^3/m^3).*

ends to chloride solution, which is the condition in the performed experiments. The symmetry in the geometry and in applied boundary conditions allows for setting the flow to zero at the middle of the one-dimensional domain of interest. Hence, due to symmetry, only the half of the one-dimensional domain is studied in the simulation.

The bulk water values of the diffusion coefficients and ionic mobilities are given in Table 1. The bulk diffusion values are scaled with the tortuosity factors presented in Table 11. The use of the material coefficients presented in Table 11, was shown to give the best fit with the measured chloride profiles, for the three studied concrete qualities, see Figures 1-3.

The physical meaning of all introduced constants is explained in sections 3 and 4. The binding rates of Cl^- and OH^- were set to the same value for all three concrete qualities tested, and furthermore, the binding capacity of OH^- was set to the same value for the three studied concrete qualities. The

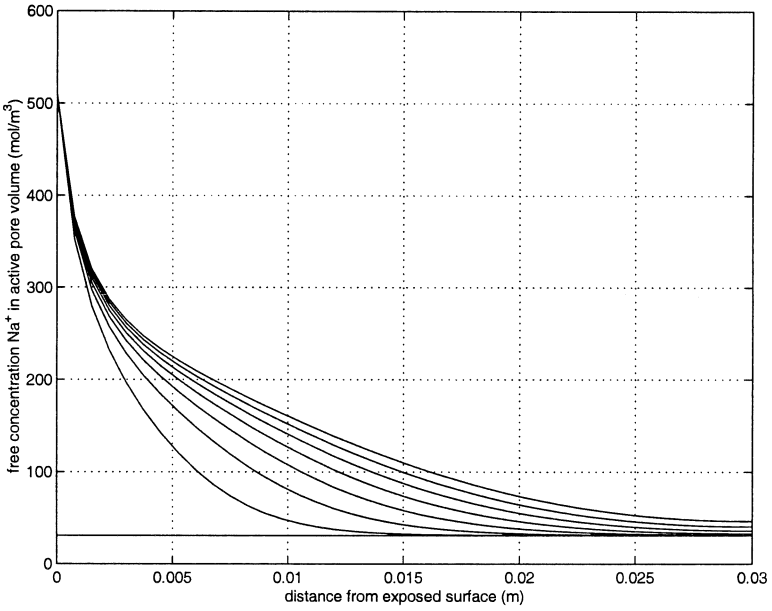

Figure 5: *Calculated free concentration of dissolved sodium ions in active pore volume for the SRPC concrete with 5% silica fume, w/b 0.55. The profiles represent exposure up to 119 days. The time step length between profiles is 17 days (profiles develop from left to right). The active water filled porosity is measured as 0.107 (m^3/m^3).*

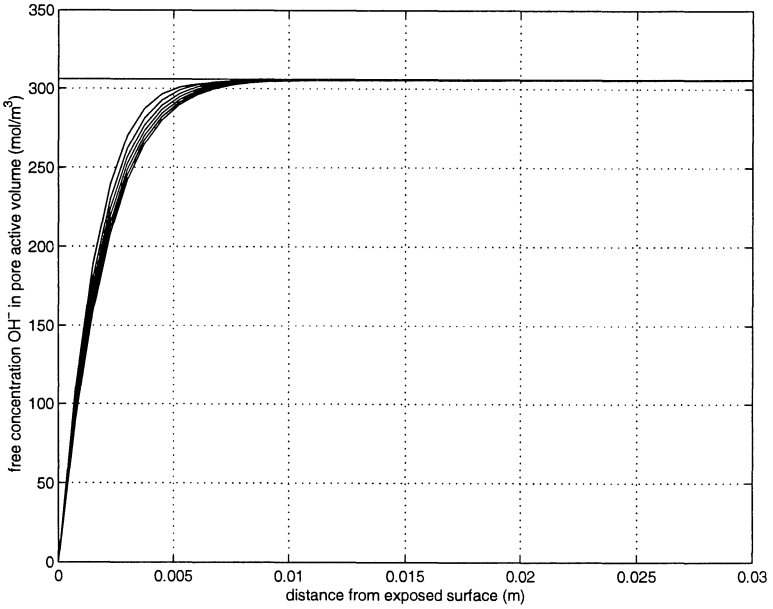

Figure 6: *Calculated free concentration of dissolved hydroxide ions in active pore volume for the SRPC concrete with 5% silica fume, w/b 0.55. The profiles represent exposure up to 119 days. The time step lenght between profiles is 17 days (profiles develops from left to right). The active water filled porosity is measured to be 0.107 (m^3/m^3).*

numerical values of these constants were chosen so as to get the best average fit for the three concrete qualities. The parametric study is therefore based on adjustment of the tortuosity factor (which is assumed to be the same for all studied types of ions present in pore solution) and the binding capacity of chloride ions.

The conclusion drawn from the simulation is that the tortuosity is very little affected by the different water to binder ratios in use. The ratio of the lowest and highest value obtained was 0.92, i.e. 0.00516/0.00561, compare Table 11. On the other hand, the ratio of the lowest and highest value of the binding capacity of chloride ions obtained was 0.16, i.e. 0.36/2.22. There are many possible reasons for these results. One is the definition used for the active water-filled porosity, in which dissolved ions can appear. This will affect the value of the binding capacities since they are related to the concentration of ions in pore solution. Another possible reason is that the preconditioning

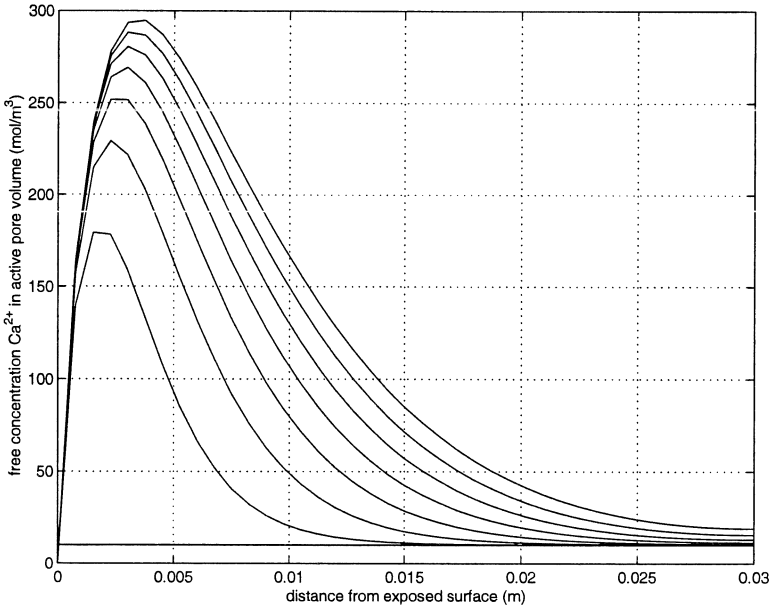

Figure 7: *Calculated free concentration of dissolved calcium ions in active pore volume for the SRPC concrete with 5% silica fume, w/b 0.55. The profiles represent exposure up to 119 days. The time step length between profiles is 17 days (profiles develop from left to right). The active water filled porosity is measured as 0.107 (m^3/m^3).*

of the cast samples, which consisted of drying for two weeks followed by re-wetting for one week using tap water, affects the micro-structure. According to the results from simulation, drying at early ages can be one cause contributing to the observation that the tortuosity effect becomes similar for the different tested water to binder ratios, i.e. drying and re-wetting makes the micro-structure similar for all water to binder ratios with respect to diffusion. Considering the binding capacity, the specific surface area may be changed, due to drying at early ages, contributing to great differences in the capacity for chloride binding between the tested water to binder ratios.

By including dielectric effects among ions in pore solution, the normally observed occurrence of a maximum total chloride content in concrete a few millimeters depth from the exposed surface, can be modeled theoretically, compare measured values and simulated results shown in Figures 1-3. This can hardly be modeled when assuming the diffusion to be dependent on the

Table 11: Material constants used for the three different concrete mixes based on SRPC with 5 percent silica fume. The samples were dried for two weeks and re-wetted for one week before exposure to a 3 weight percent sodium chloride solution. The constants presented are the ones giving the best fit with the measured total chloride profiles when used in the proposed model.

Material constants	w/b 0.35	w/b 0.40	w/b 0.55
Tortuosity factor, (-)	0.00516	0.00550	0.00561
Binding cap., Cl^-, $1/K$ (-)	2.22	1.25	0.36
Binding rate, Cl^-, R (1/s)	0.0012	0.0012	0.0012
Binding cap., OH^-, W (-)	0.0102	0.0102	0.0102
Binding rate, OH^-, Q (1/s)	$1 \cdot 10^{-6}$	$1 \cdot 10^{-6}$	$1 \cdot 10^{-6}$
Measured active porosity	0.0562	0.0788	0.1073

concentration gradient of ions alone, as assumed in most existing models for chloride transport.

The results from the simulation, in terms of other calculated concentrations than total chloride profiles, at different time levels, are presented in Figures 4-10. Only results from the concrete quality with water to binder ratio 0.55 are presented. The total chloride profile shown in Figure 3 constitutes the sum of the free concentration of ions in pore solution, see Figure 4, and ions being incorporated in solid calcium chlorides, see Figure 9. It is seen, from figure 4, that the model simulates that the free concentration of chlorides in pore solution, near the exposed surface, is higher than the outer storage solution, which is 510 mol/m^3. This is caused by dielectric effects among different types of ions included in the model. Further, it is seen, from Figure 5, that the ingress of sodium ions in pore solution is heavily damped compared to the ingress of free chlorides, i.e. compare Figure 4 and 5. The conclusion is that sodium ions and chloride ions, supplied from the storage solution, do not follow each other when penetrating the water-filled pore system, which means that other types of ions, included in the model, than sodium and chloride ions are involved, making the net charge of the pore solution equal to zero. The dissolution of hydroxide ions from pore solution to storage solution was shown to be small according to the simulation, see Figure 6. It was a depth from the exposed surface of, approximately 5 mm that was affected by this leaching. On the other hand, the calculated leaching of dissolved potassium ions in pore solution was high, see Figure

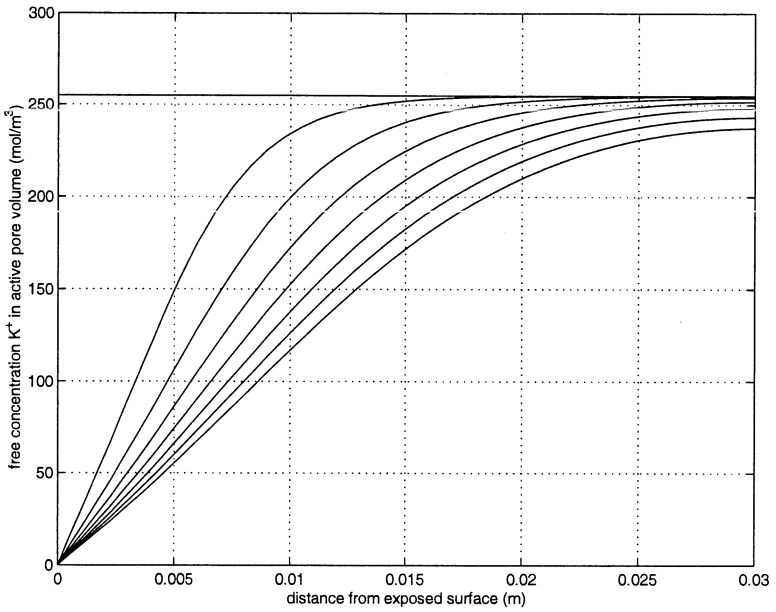

Figure 8: *Calculated free concentration of dissolved potassium ions in active pore volume for the SRPC concrete with 5% silica fume, w/b 0.55. The profiles represent exposure up to 119 days. The time step length between profiles is 17 days (profiles develop from left to right). The active water filled porosity is measured as 0.107 (m^3/m^3).*

8. The calcium ion concentration in pore solution, at different times from exposure, is shown in Figure 7. These concentrations profiles have their maximum at depths ranging from 2 to 4 mm. The considerably high values for calcium ions in the domain is, apart from diffusion and dielectrical effects, due to the assumed dissolution of calcium caused by the chemical reaction (19). The obtained values, in terms of concentration profiles, for the two solid constituents calcium chloride and calcium hydroxide are presented in figures 9 and 10. For computational convenience, these values are defined as mol densities, as related to the water-filled pore volume.

Two different measures of the effective diffusion constants are calculated. The first, D_{eff}, is the most common used 'effective' diffusivity which is obtained by fitting the solution of Fick's second law to the measured total chloride profile taken at a certain time from start of exposure. No special attention is paid in this method to the really occurring boundary condition,

Table 12: Two different measures of the effective diffusion constant for chlorides. Samples were exposed to a 3 weight percent sodium chloride solution for 119 days.

Concrete mix	D^*_{eff} (m^2/s)	D_{eff} (m^2/s)
w/b 0.35	$1.92 \cdot 10^{-12}$	$1.24 \cdot 10^{-12}$
w/b 0.40	$3.19 \cdot 10^{-12}$	$1.73 \cdot 10^{-12}$
w/b 0.55	$6.64 \cdot 10^{-12}$	$3.68 \cdot 10^{-12}$

in terms of chloride ion concentration. The solution is rather fitted to the total chloride content profile where concentrations measured near the exposed surface are ignored. This is, of course, a very rough approximation. The values of D_{eff} obtained by the above described method are presented in Table 12, for the three examined concrete qualities.

The obtained D_{eff} values are compared with values denoted D^*_{eff} which are calculated from results given from the simulation performed. The D^*_{eff} value is calculated by the formula: $D^*_{eff} = \tilde{D}_1/(1+2K^{-1})$, where $\tilde{D}_1$ is the scaled diffusion constant for free chloride ions in the pore system and K is described in section 4. This formula can be derived by considering a 'standard' diffusion equation with mass exchange as: $\partial\rho_{cl}/\partial t = \tilde{D}_1\partial^2\rho_{cl}/\partial x^2 - \partial\rho^b_{cl}/\partial t$, where $-\partial\rho^b_{cl}/\partial t$ is the mass exchange rate between dissolved chlorides in pore solution and bound chlorides. The mass concentration of bound chlorides is denoted ρ^b_{cl} and the free chloride concentration with ρ_{cl}. Assume also a binding isotherm given as: $\rho^b_{cl} = 2K^{-1}\rho_{cl}$. That is, a given one-to-one relation between the mass concentration of free chlorides in pore solution and bound chlorides is assumed valid under all conditions. Combining the above two assumed relations, one obtains: $\partial\rho_{cl}/\partial t = \tilde{D}_1/(1+2K^{-1})\,\partial^2\rho_{cl}/\partial x^2$. It is concluded that a high binding capacity reduces the effective diffusion constant D^*_{eff}, and the penetration rate, therefore, becomes small in this case.

The difference between the binding isotherm $\rho^b_{cl} = 2K^{-1}\rho_{cl}$ and the equilibrium condition $n_1^{eq} = Kn_6$, described in section 4 (in which $Z = 0$ is used), is due to the use of mol concentration instead of mass density relations.

As seen in Table 12, the values of D_{eff} and D^*_{eff} differ significantly. This is mainly caused by not accounting for the measured concentration values near the exposed surface when evaluating D_{eff}.

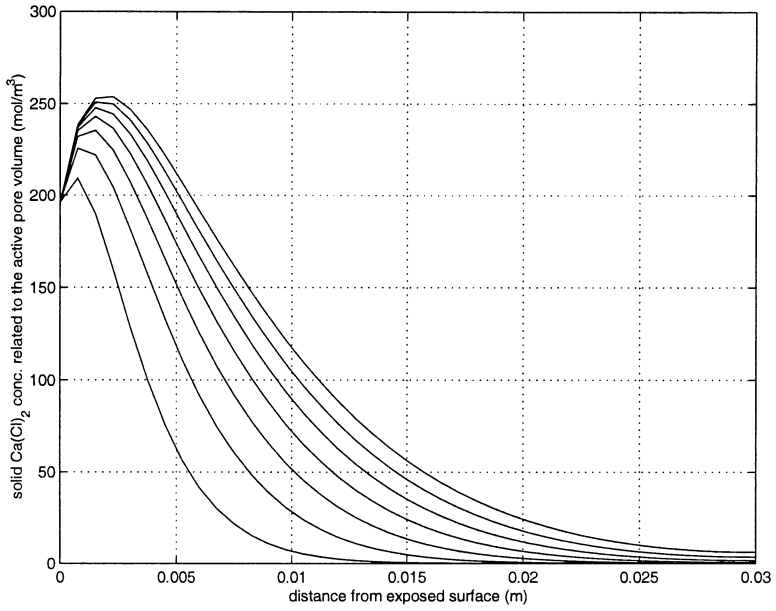

Figure 9: *Calculated concentration of solid calciumchloride as related to the active pore volume, SRPC concrete with 5% silica fume, w/b 0.55. The profiles represent exposure up to 119 days. The time step length between profiles is 17 days (profiles develop from left to right). The active water filled porosity is measured as 0.107 (m^3/m^3).*

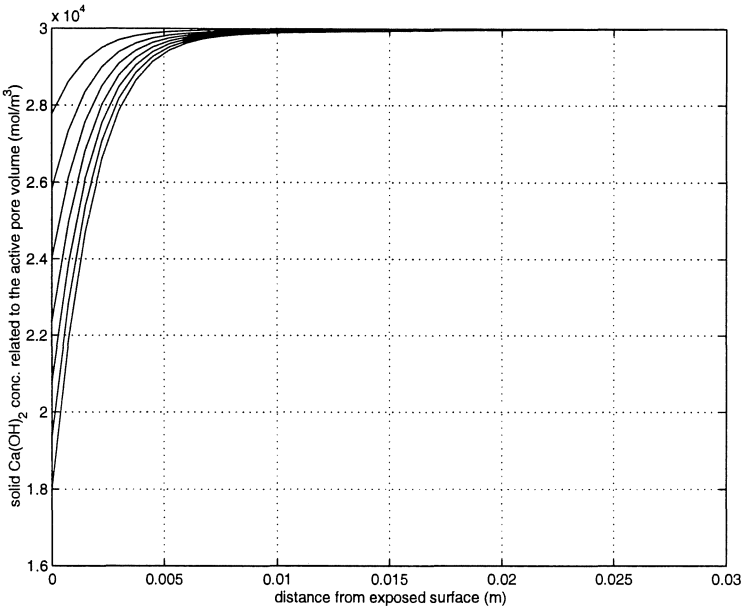

Figure 10: *Calculated concentration of solid calciumhydroxide as related to the active pore volume, SRPC concrete with 5% silica fume, w/b 0.55. The profiles represent exposure up to 119 days. The time step length between profiles is 17 days (profiles develop from left to right). The active water filled porosity is measured as 0.107 (m^3/m^3).*

9 Possible improvements of the model

Naturally, there are several different possibilities to improve the discussed model. The most important issue is perhaps to include several more constituents and also use a more detailed description of the chemical reactions taking place in such a system. It is also realized that the solution of the presented equations, including just a few constituents, becomes quite involved. For example, non-linearities in the chloride-binding isotherm can be incorporated by letting the K-value be a function of the concentration of bound chlorides. The effect of hydroxide ion concentration in the pore solution on chloride binding can be studied by including the constant Z as described in section 4. The comparison between the obtained experimental results and simulated response in this paper did not, however, indicate that these effects are dominant, since a satisfying match between simulations and the experimental data was obtained. Experimental data on equilibrium chloride binding isotherms, using pore pressing, shows that the binding isotherm indeed is non-linear at relatively high free chloride concentrations for some concrete qualities. This is a contradictory result as compared with the experiments and simulation performed in this work.

The needed experimental data involves determination of concentration profiles of all considered constituents at different times from exposure. Since the chloride ion profiles are the only experimental data used to match the material parameters in the model described, it is important to extend the work performed so far with several experiments. In light of this fact, the experimental and theoretical conclusions from this study must be seen as a preliminary attempt to establish a closed set of equations describing the behavior of the condition of the pore solution of concrete.

The model does, indeed, handle arbitrary variations of boundary conditions in terms of concentrations of different types of ions. It should be observed, however, that the effect of convection of ions caused by capillary suction is ignored for reasons of simplicity. This problem has been studied experimentally [24], theoretically [29] and numerically [30] for concrete exposed to capillary suction and chlorides. This concept has, however, never been combined with the effect of dielectrics among positive and negative ions present in pore solution. It is important to deal with this problem since many of the most severe conditions consist of concrete constructions being exposed to de-icing salts altered by intermittent drying periods.

Another important phenomenon ignored in this study are the solubilities

of the different types of ions present in the pore solution. These properties must be studied by considering all different types of ions dissolved in pore solution. It is possible that the calculated concentrations of ions, in the model used, is unrealistic since it does not account for precipitation of neutral combinations of ions in certain conditions. The precipitation properties for the studied mixture of ions can be studied by simple direct experimental methods or with theoretical considerations using the concept of ionic strength.

The numerical solution to the non-linear problem of interest can be improved by using a sophisticated method when it comes to making 'out of balance' minimizations. This method must be able to tackle non-symmetrical properties of the global 'stiffness' matrix.

10 Conclusions

It is concluded that the effect of the composition of the mixture of ions on the diffusion characteristics of the individual dissolved ion types is an important issue when dealing with chloride penetration into cement-based materials. It is shown in the paper that the requirement that dissolved ions should diffuse through the pore system in a way that the net charge at every material point and at every time level is very close to zero gives one possible explanation for obtaining the normally experimentally observed enrichment of chlorides near the exposed surface. By accounting for the dielectic effects it was possible to obtain a fairly good match between chloride profiles obtained by simulation and experiments. It should be carefully observed, however, that other mechanisms than the ones assumed here may be the cause of the measured response in terms of chloride ingress. In order to study this, other kinds of constitutive assumptions must be tested.

The assumed values of the diffusion coefficients and ion mobility coefficients for the different types of ions in pore system had to be small for the lowest water to binder ratios tested, and a comparably high value had to be used for the highest water to binder ratio, in order to get a good correlation between the calculated and experimentally obtained data. This is presumably caused by a higher tortuosity effect for the concrete with low water to cement ratio. Further, the assumed equilibrium conditions between bound chloride and dissolved chloride had to be higher for concretes having a higher cement content in the mix, in order to match the governed equations with the experimental data. These results are what could be expected.

The results from the simulation showed that leaching of hydroxide ions in pore solution into the outer storage solution was small, see Figure 6. At greater depths than 10 mm no leaching occurred. This is due to a combined effect of (*i*) the assumed dissolution rate of calcium and hydroxide ions from solid calcium hydroxide, as described by equation (19), and (*ii*) properties affecting diffusion of hydroxide ions in pore solution, i.e. concentration gradient dependent diffusion and (*iii*) effects on diffusion caused by dielectrics among different types of ions. The behavior also is dependent on the buffer of solid calcium hydroxide in concrete which is assumed to be high in the simulation made, compare Figure 10.

On the other hand, the simulation indicates an enrichment of calcium ions in pore solution in the whole domain with a maximum approximately at the depth 4 mm, after 119 days of exposure, see Figure 7. This behavior is, again, due to the assumed dissolution reaction (19) and the rate of diffusion of calcium ions to outer storage solution and dielectric effects. It is the resulting shape of the calcium ions profiles in pore solution, shown in Figure 7, which forces the chloride ions to be enriched near exposed surface. Loosely speaking, the chloride ions are forced to level out the electrical inbalance caused by calcium ions entering the pore solution due to dissolution of solid calcium hydroxide. It is also noted by the simulation that dissolved hydroxide ions cannot compensate for this behavior.

In order to verify the described model for diffusion and chemical reactions of ions in the pore solution of cement-based materials, an experimental determination of concentration profiles of all considered ions must be performed for given exposure conditions. In this work only the experimentally obtained chloride profiles were studied together with a model including several types of ions, besides chlorides. Further, one of the main issues is to find the relations of solubility properties of ions in the considered system of constituents.

It is also concluded that the method for dividing the total chloride content in two parts, one part being dissolved in pore solution and the other being bound, is very crucial. This makes possible a scaling of the diffusion coefficient valid for ions in bulk water with a tortuosity factor accounting for the shape of the micro-structure. Further, this way of dividing the total concentration of chloride ions means that the effects caused by electrical forces among the positive and negative ions in pore solutions can be studied theoretically in a stringent manner.

References

[1] Bowen, R.M. (1976). *Theory of Mixtures*, Part 1, in Continuum Physics, Edited by A. Cemal Erigen, Princeton University of Technology.

[2] Johannesson, B.F. (1998). *Modelling of Transport Processes Involved in Service Life Prediction of Concrete, Important Principles*, Division of Building Materials, Lund University of Technology.

[3] Weast, R.C., Lide, D.R. Astle, M.J. and Beyer, W.H. (1989). *Handbook of Chemistry and Physics*, 70^{TH} edition, CRC Press, Inc. Boca Raton, Florida.

[4] Atkins, P.W. (1994). *Physical Chemistry*, Fifth Edition, Oxford University Press, Oxford.

[5] Castellote, M., Andrade, C. and Cruz Alonso, M. (1999). *Changes in Concrete Pore Size Distribution Due to Electrochemical Chloride Migration Trials*, ACI Materials Journal, V. 96, No. 3, pp. 314-319.

[6] Sharif, A. A., Loughlin K.F. Azad, A.K. and Navaz, C.M. (1997). *Determination of the Effective Chloride Diffusion Coefficient in Concrete via a Gas Diffusion Technique*, ACI Materials Journal, V. 94, No. 3, pp. 227-233.

[7] Samson, E., Marchand, J. and Beaudoin, J.J. (1999). *Describing ion diffusion mechanisms in cement-based materials using the homogenization technique.* Cement and Concrete Research, V. 29, pp. 1341-1345.

[8] Martys, N.S. (1999). *Diffusion in Partially-Saturated Porous Materials.* Materials and Structures, V. 32, pp. 555-562.

[9] Glass, G.K., Hassanein, N.M. and Buenfeld, N.R. (1997). *Neural Network Modelling of Chloride Binding.* Magazine of Concrete Research, V. 49, No. 181, pp. 323-335.

[10] Birnin-Yauri, U.A. and Glasser, F.P. (1998). *Friedel's Salt,* $Ca_2Al(OH)_6\,(Cl, OH) \cdot 2H_2O$*: its Solid Solutions and their Role in Chloride Binding*, Cement and Concrete Research, V. 28, No. 12, pp. 1713-1723.

[11] Wee, T.H., Wong, S.F., Swaddiwudhipong, S. and Lee, S.L. (1997). *A Prediction Method for Long-Term Chloride Concentration Profiles in Hardening Cement Matrix Materials.* ACI Materials Journal, V. 94, No. 6, pp. 565-579.

[12] Sandberg, P. (1995). *Critical Evaluation of Factors Affecting Chloride Initiated Reinforcement Corrosion in Concrete*, Division of Building Technology, Lund Institute of Technology.

[13] Tritthart, J. (1992). *Changes in Pore Water Composition and in Total Chloride Content at Different Levels of Cement Paste Plates Under Different Storage Conditions*, Cement and Concrete Research. Vol. 22, pp. 129-138.

[14] Sergi, G., Yu, S.W. and Page, C.L. (1992). *Diffusion of Chloride and Hydroxyl Ions in Cementitious Materials Exposed to a Saline Environment*, Magazine of Concrete Research. 1992, Vol. 44, No. 158, Mar., pp. 63-69.

[15] Page, C.L., Lambert, P. and Vassie, P.R.W. (1991). *Investigations of Reinforcement Corrosion. 1. The Pore Electrolyte Phase in Chloride-Contaminated Concrete,* Materials and Structures, Vol. 24, No. 139, pp. 234-252.

[16] Glass, G.K. and Buenfeld, N.R. (1995). *The Determination of Chloride Binding Relationships*, Chloride Penetration into Concrete, Proceedings of the International Rilem Workshop, St-Rémy-lès-Chevreuse, France.

[17] Midglay, H.G. and Illston, J.M. (1984). *The Penetration of Chlorides into Hardened Cement Pastes,* Cement and Concrete Research. Vol. 14, pp. 546-558.

[18] Sandberg, P. (1996). *Durability of Concrete in Saline Environment*, Cementa AB, Sweden.

[19] Tritthart, J. (1989). *The Influence of the Hydroxide Concentration in the Pore Solution of Hardened Cement Pastes on Chloride Binding*, Cement and Concrete Research. Vol. 19, pp. 683-691.

[20] Ottosen, N.S. and Petersson, H. (1992). *Introduction to the Finite Element Method*, Prentice Hall, London.

[21] Zienkiewicz, O.C. and Taylor, R.L. (1989). *The Finite Element Method, Fourth Edition, Vol. 2*, McGraw-Hill, London.

[22] Bathe, K.J. (1996). *The Finite Element Procedures*, Prentice Hall, Englewood Cliffs, New Jersey.

[23] Hughes, T.J.R. (1987). *The Finite Element Method, Linear Static and Dynamic Finite Element Analysis,* Prentice-Hall International Editions.

[24] Janz, J. and Johannesson, B.F. (1993). *A Study of Chloride Penetration into Concrete* (in Swedish), Division of Building Technology, Lund University of Technology.

[25] *Chloride Penetration into Concrete*, Proceedings of the International Workshop St. Rémy-lès-Chevreuse, France, 15-18 October 1995, Edited by Lars Olof Nilsson and Jean-Pierre Ollivier (RILEM Publications, France).

[26] *Corrosion of Reinforcement, Field and Laboratory Studies for Modelling and Service Life*, Proceedings of the Nordic Seminar in Lund, Sweden, 1-2 February 1995, Edited by Kyösti Tuutti, Division of Building Technology, Lund University of Technology.

[27] Lindmark, S. (1998). *Mechanisms of Salt Frost Scaling of Portland Cement-bound Materials: Studies and Hypothesis* (Doctoral Thesis), Division of Building Materials, Lund University of Technology.

[28] RCT, Instructional and Maintenance Manual. (1998). Germann Instrument A/S, Copenhagen, Denmark.

[29] Johannesson, B.F. (1997). *Nonlinear Transient Phenomena in Porous Media with Special Regard to Concrete and Durability*, Advanced Cement Based Materials, Vol. 6, pp. 71-75.

[30] Johannesson, B.F. (1996). *Convection-diffusion Problems with Significant First-order Reversible Reactions*, Ninth Nordic Seminar on Computational Mechanics, Technical University of Denmark, Department of Structural Engineering and Materials, Edited by Lars Damkilde, pp. 231-236.

LUNDS TEKNISKA
HÖGSKOLA
Lunds universitet